# Mammalian glial protrusion transcriptomes predict localization of *Drosophila* glial transcripts required for synaptic plasticity

DALIA S. GALA[1*], JEFFREY Y. LEE[1*], MARIA KIOURLAPPOU[1], JOSHUA S. TITLOW[1], RITA O. TEODORO[2], ILAN DAVIS[1]

## Authors institutional affiliations

1 Department of Biochemistry, The University of Oxford, UK

2 NOVA Medical School - Faculdade de Ciências Médicas, Universidade Nova de Lisboa, Portugal

* these authors contributed equally to the work

## SUMMARY (150 words)

The polarization of cells often involves the transport of specific mRNAs and their localized translation in distal projections. Neurons and glia both contain long cytoplasmic processes with important functions. While mRNA localization has been studied extensively in neurons, little is known in glia, especially in intact nervous systems. Here, we predicted 1700 localized *Drosophila* glial transcripts by extrapolating from our meta-analysis of 8 existing studies characterizing the localized transcriptomes and translatomes of synaptically-associated mammalian glia. We tested these predictions in glia of the neuromuscular junction of *Drosophila* larvae and found that localization to vertebrate glia is a strong predictor of mRNA localization of the high confidence *Drosophila* homologues. We further showed that some of these localized transcripts are required in glia for plasticity of neuromuscular junction synapses. We conclude that peripheral glial mRNA localization is a common and conserved phenomenon and propose that it is likely to be functionally important.

## KEYWORDS:

*Drosophila*, glia, mRNA transport, mRNA, mRNA localization, localized translation

# 1 INTRODUCTION

Most cells are polarized, where different cellular regions possess distinct functional domains, often with specialized structural adaptations. Usually, polarization is reflected in asymmetrical morphology, prominent in the cells composing the nervous system, such as neurons and glia, which exhibit numerous and complex processes. These cell types maintain unique subcellular environments through protein trafficking, or by mRNA localization and local translation as a more rapid means of producing protein at the site of function.

Multiple studies found mRNAs actively transported and enriched in distal compartments of neurons, including those encoding cytoskeletal proteins, neurotransmitters, membrane proteins and ribosomes. In these studies, mRNA transport and local translation have been proposed as mechanisms for local regulation of synaptic plasticity, which is the process underlying memory and learning (Smith, Aakalu and Schuman, 2001; Sutton and Schuman, 2006; Wang, Martin and Zukin, 2010; Daniel E Shumer, 2017; Rangaraju, tom Dieck and Schuman, 2017; Terenzio, Schiavo and Fainzilber, 2017; Biever, Donlin-Asp and Schuman, 2019; Holt, Martin and Schuman, 2019).

Despite being less studied, asymmetric mRNA localization is likely to be equally important in glia. Like neurons, glial cells can display a range of morphologies ranging from immune-cell-like microglia, to elongated myelinating oligodendrocytes and Schwann cells. Perhaps most dramatic are astrocytes that contact hundreds to thousands of synapses belonging to different neurons through equally many elongated processes, and therefore have a tremendous potential to integrate information from distinct neuronal populations (Ransom and Ransom, 2012; Jessen, Mirsky and Lloyd, 2015; Allen and Lyons, 2018; Volterra and Meldolesi, 2005). Recent research has identified many of these glial subtypes as more active and involved in synaptic plasticity than previously thought. Astrocytes, for example, perform key roles in the uptake and release of neurotransmitters and the maintenance of ionic balance. They are also essential for forming the blood-brain barrier which regulates neuronal metabolism and local solute homeostasis, as well as for secretion of gliotransmitters and mediation of signaling pathways (De Pittà, Brunel and Volterra, 2016; Wang, Fu and Ip, 2022; Ota, Zanetti and Hallock, 2013).

Oligodendrocytes are thought to modulate synaptic plasticity via myelination (Fields, 2005; Fields, 2008; de Faria *et al.*, 2021; Bacmeister *et al.*, 2020; Pan *et al.*, 2020; Fields and Bukalo, 2020). Microglia can preferentially phagocytose synaptic endings and modulate connectivity in the visual cortex (Andoh and Koyama, 2021; Graeber, 2010; Morris *et al.*, 2013; Schafer *et al.*, 2012; Vasek *et al.*, 2021). Although these varying glial morphologies and roles are suggestive of mRNA localization, like they are in neurons, little is known about local translation in glial cytoplasmic processes. In recent years, there has been an increased interest in this topic, but glial roles in nervous system function and development are still far from being fully understood (Blanco-Urrejola *et al.*, 2021; Meservey, Topkar and Fu, 2021). It is not clear whether a common set of mRNAs exists that localizes to the periphery of most of the glial sub-types or in neurons, nor is it known whether such glial mRNA localization is conserved and functionally important.

To address these questions, we have carried out a meta-analysis of, to our knowledge, all the published mammalian glial peripheral or synaptic transcriptomes and translatomes. We found several classes of mRNAs that are localized in multiple glial subtypes and determined a common set of 4801 transcripts present in the majority of the analyzed libraries, representing multiple types of mammalian glial cells. We used this cohort to find high confidence *Drosophila* homologues and filtered the list for glial expression using the Fly Cell Atlas data, a single-cell nuclear sequencing atlas derived from entire adult flies (Li *et al.*, 2022). For our filtering, we specifically selected the 3 glial subtypes known to create distal protrusions in the larval NMJ, which are perineural, subperineural and wrapping/ensheathing glia (Yildirim *et al.*, 2019; Sepp, Schulte and Auld, 2000). This query produced 1700 mRNAs predicted to be localized in these three glial subtypes. To confirm our prediction of mRNA localization, we utilized single molecule Fluorescence *In Situ* Hybridisation (smFISH) experiments and surveyed transcripts that were previously reported to be present in the *Drosophila* NMJ glia (Titlow *et al.*, 2022). These smFISH experiments revealed that more than 70% of the localized transcripts matched our prediction, demonstrating utility of our dataset. Furthermore, we found that specific knockdown of localized transcripts in glia can affect synaptic plasticity of the adjacent wild-type neuron, as measured by spaced potassium stimulation assay (Ataman *et al.*, 2008; Roche *et al.*, 2002). We showed that knockdown of 30% of

these predicted transcripts impaired synaptic plasticity in the neighboring neuron and caused morphological defects of the NMJ synapses. Our results suggest that mRNA localization to protrusions may represent an important and possibly conserved mechanism that allows glia to rapidly regulate the plasticity of adjacent distal axonal synapses.

# 2 MATERIALS AND METHODS

## 2.1 Data meta-analysis methods

We developed a custom RNA-seq analysis pipeline to process public transcriptomic datasets and allow the integration of diverse raw datasets from 8 different studies. Raw FASTQ files were downloaded from Gene Expression Omnibus (GEO) and were filtered to remove ribosomal RNA reads using BBduk (Bushnell, Rood and Singer, 2017). Processed reads were mapped to *Mus musculus* (ENSEMBL release 96) or *Rattus norvegicus* (ENSEMBL release 98) genomes using Kallisto to obtain Transcripts per million (TPM) abundance measures (Bray *et al.*, 2016). A TPM value > 10 for a transcript was considered a transcript to be present in a given compartment. In order to take into account intronic reads in libraries derived from soma, Kallisto bustools was used to create transcriptome indices containing intron sequences (Melsted *et al.*, 2021). For the relative enrichment analysis comparing soma and protrusion compartments, DESeq2 was used to assess differential expression of transcripts from estimated transcript counts output (Love, Huber and Anders, 2014). The independent hypothesis weighting (IHW) method was used to correct for the multiple testing (Ignatiadis *et al.*, 2016), and the adjusted p-value<0.01 & log2FoldChange>0 was considered significantly enriched.

For the datasets where raw data were unavailable, the reported HTSeq count table was used as input for DESeq2, and the conflicting transcript annotations between ENSEMBL releases were manually resolved. In the case of non-Illumina-based sequencing datasets, numerical log2foldchange was calculated from the reported TPMs of each gene. *R. norvegicus* datasets were converted to *M. musculus* genes using ENSEMBL BioMart annotations after the differential expression processing. All summary data obtained from our analysis is available in Supplementary Table 1.

Gene Ontology (GO) enrichment analyses were performed using a Bioconductor package TopGO (Alexa and Rahnenfuhrer, 2022). To prevent artefactual enrichment of brain-related terms, adult mouse brain transcriptome (Accession number: ENCFF468CXD) from ENCODE project was used as background. Multiple testing was corrected via the Bonferroni method. An adjusted p-value<0.05 and foldchange>2 was considered a significant enrichment. Summaries of enriched GO terms were processed using the R package SimplifyEnrichment (Gu and Hübschmann, 2022) via clustering significantly enriched GO terms based on semantic similarity. Unclustered individual GO terms are given in Figure S2 and Supplementary Table 2

Conversion between human, mouse and fly orthologues (ENSEMBL release 99) was performed using the source data of DIOPT version 9 (Hu *et al.*, 2011). To select for high-confidence orthologues, a cut-off score of 8 was used. Fly genes with the associated disease ontologies were acquired from FlyBase, and the enrichment of disease ontology terms were assessed with hypergeometric test followed by Bonferroni's method multiple hypothesis correction.

To identify transcripts that are expressed in the three glial cell types (perineurial, subperineurial and ensheathing glial cells), single-cell nucleus sequencing data from Fly Cell Atlas was used (Li *et al.*, 2022). 'Glial Cell' loom file from 10x Cross-Tissue dataset was downloaded and filtered for non-glial cells based on the annotation. Using the R package ScopeLoomR (https://github.com/aertslab/SCopeLoomR), the digital gene expression matrices for the three cell types were extracted and the transcripts expressed in at least 5% of the corresponding clusters were identified.

For the Reactome pathway enrichment analysis, the gene to pathway query from Flymine was used to extract the Reactome ID annotations for each gene (https://www.flymine.org/flymine/templates/Gene_Pathway). The Reactome pathway hierarchical relationship between terms (available here) was used to group genes to the two highest hierarchical levels, the "top-level pathways" and the next hierarchical level, the "sub-pathways", was used to calculate the enrichment.

All analysis scripts and data produced from this study are available at https://github.com/jefflee1103/Gala2023_glia-localised-RNA. The data that supports the findings of this study are available in the supplementary material of this article.

## 2.2 Experimental methods

### 2.2.1 Fly stocks

The fly lines used in this research were raised at 25ºC (all stocks used in the smFISH experiments and the spaced potassium assay experiment apart from *Nrg*-RNAi) or 30ºC (larvae used for the *Nrg*-RNAi spaced potassium assay experiment in glial cells) on a standard cornmeal-agar food. To label glial cells in the smFISH experiments, a cross was made to obtain the following stock: UAS-mCD8-mCherry/CyoGFP; Repo>GAL4/Tm6B, Tb. This stock was then crossed to each of the CPTI lines and offspring selected for YFP and mCherry fluorescence. To label glia in the spaced potassium assay experiment with RNAi of transcripts of interest in glial cells, the following stock was constructed: UAS-mCD8-GFP/UAS-mCD8-GFP; Repo>GAL4/Tm6B, Tb. For each RNAi experiment, a homozygous line where hairpin targets the coding sequence of the gene of interest with least number of off-targets was selected. If the progeny of the RNAi cross was embryonic or larval lethal, the next best RNAi line was used. These lines were then crossed to the UAS-mCD8-GFP/UAS-mCD8-GFP; Repo-GAL4/Tm6B, Tb, and offspring selected for GFP fluorescence and lack of Tm6B, Tb phenotype. The control for the UAS-RNAi experiment was UAS-mCD8-GFP/+; Repo-GAL4/UAS-mCherry-RNAi. The glial cell specific knockdown of the 11 localized transcripts resulted in lethality for *Cip4*, where no 3rd instar Drosophila larvae of the correct genotype were observed. For Atpalpha (GD3093) and *Lac* (KK107450), the UAS-RNAi larvae were extremely few, small and sickly, and the experiments could not be performed on them. Using other UAS-RNAi lines for *Atpalpha* (HMS00703) and *Lac* (GD35524) allowed us to continue with experiments on those knockdown larvae. We observed no adults of the UAS-RNAi genotype for *nrv2*-RNAi, *Lac*-RNAi, *Cip4*-RNAi, and *Vha55*-RNAi. We observed adults for all other Repo>UAS-RNAi. crosses. **Table 1** lists all the strains used in the study.

| Line name | Line ID | Line source | Line description |
|---|---|---|---|
| *nrv2*::YFP | CPTI001455 | Kyoto Stock Centre - Drosophila Genomics and Genetic Resources (DGRC) (https://www.dgrc.kit.ac.jp/) | *Nervana 2* gene YFP protein trap line ((Lowe *et al.*, 2014) |
| *Flo-2*::YFP | CPTI001427 | DGRC | *Flotillin 2* gene YFP protein trap line |
| *Cip4*::YFP | CPTI003231 | DGRC | *Cdc42-interacting protein 4* gene YFP protein trap line |
| *Vha55*::YFP | CPTI002645 | DGRC | *Vacuolar H+-ATPase 55kD subunit* gene YFP protein trap line |
| *Atpalpha*::YFP | CPTI002636 | DGRC | *Na pump α subunit* gene YFP protein trap line |
| *Nrg*::YFP | CPTI002761 | DGRC | *Neuroglian* gene YFP protein trap line |
| *Lac*::YFP | CPTI001714 | DGRC | *Lachesin* gene YFP protein trap line |
| *alpha-Cat*::YFP | CPTI002408 | DGRC | *α Catenin* gene YFP protein trap line |
| *Pdi*::YFP | CPTI002342 | DGRC | *Protein disulfide isomerase* gene YFP protein trap line |
| *gs2*::YFP | CPTI001918 | DGRC | *Glutamine synthetase 2* gene YFP protein trap line |
| Repo-GAL4 | RRID:BDSC_7415 | Bloomington Drosophila Stock Center (BDSC) (https://bdsc.indiana.edu/index.html) | Expresses GAL4 in glia |
| UAS-mCD8-mCherry/cyo-GFP | RRID:BDSC_27391 | BDSC | Expresses Cherry RFP fused to the mouse CD8 extracellular and transmembrane domains for membrane targeting under UAS control. |
| UAS-mCD8-GFP/cyo-GFP | RRID:BDSC 63045 | BDSC | Expresses GFP fused to the mouse CD8 extracellular and transmembrane domains for membrane targeting under UAS control. |
| cyo-GFP/Gla; tm6, tb/pri | Crossed from BDSC stocks | BDSC | A double balanced stock carrying Cyo-GFP over Gla on the 2nd chromosome and tm6, tb over prickle on the 3rd chromosome. |
| *Atpalpha*-RNAi | RRID:BDSC 32913 | BDSC | Expresses dsRNA for RNAi of Atpalpha under UAS control in the VALIUM20 vector. |
| *Atpalpha*-RNAi | GD3093 | Vienna Drosophila Resource Center (VDRC) | Expresses dsRNA for RNAi of Atpalpha under UAS control in the pUAST vector pMF3. |
| *alpha-Cat*-RNAi | KK107298 | VDRC | Expresses dsRNA for RNAi of *alpha-Cat* under UAS control in the pUAST vector pMF3. |
| *nrv2*-RNAi | GD960 | VDRC | Expresses dsRNA for RNAi of *nrv2* under UAS control in the pUAST vector pMF3. |
| *shot*-RNAi | RRID:BDSC 28336 | BDSC | Expresses dsRNA for RNAi of shot under UAS control in the VALIUM10 vector. |
| *Vha55*-RNAi | GD 9363 | VDRC | Expresses dsRNA for RNAi of *Vha55* under UAS control in the pUAST vector pMF3. |
| *Lac*-RNAi | GD 35524 | VDRC | Expresses dsRNA for RNAi of *Lac* under UAS control in the pUAST vector pMF3. |
| *Lac*-RNAi | KK 107450 | VDRC | Expresses dsRNA for RNAi of *Lac* under UAS control in the pUAST vector pMF3. |
| *Flo-2*-RNAi | VSH 330316 | VDRC | Expresses dsRNA for RNAi of *Flo-2* under UAS control in the WALIUM20 vector. |
| *gs2*-RNAi | GD 9378 | VDRC | Expresses dsRNA for RNAi of *gs2* under UAS control in the pUAST vector pMF3. |
| *Pdi*-RNAi | GD13418 | VDRC | Expresses dsRNA for RNAi of *Pdi* under UAS control in the pUAST vector pMF3. |
| *mCherry*-RNAi | RRID:BDSC 35785 | BDSC | Expresses dsRNA for RNAi of mCherry under UAS control in the VALIUM20 vector. |

| | | | |
|---|---|---|---|
| *nrv2*-GAL4 | RRID: BDSC 6800 | BDSC | Expresses GAL4 in wrapping glia. |
| 46F-GALl4 | - | Gift from Dr. Stefanie Schirmeier | Expresses GAL4 in perineurial glia (Xie and Auld, 2011). |
| *Mdr65*-GAL4 | RRID: BDSC 50472 | BDSC | Expresses GAL4 in subperineurial glia. |

*Table 1.* List of *Drosophila melanogaster* lines which were utilized in this project.

### 2.2.2 Solutions and reagents

The Haemolymph-Like Salines (HL3 solutions) were prepared as described previously (Roche *et al.*, 2002; Ataman *et al.*, 2008). The list of all the solutions used is given below (**Table 2**).

| **Solution** | **Composition** |
|---|---|
| HL3 0.3 mM $Ca^{2+}$+ | NaCl 70 mM, KCl 5 mM, $MgCl_2$ 20 mM, $NaHCO_3$ 10 mM, trehalose 5 mM, HEPES 5 mM, sucrose 115 mM, $Ca^{2+}$ 0.3 mM, pH 7.2 |
| HL3 1 mM $Ca^{2+}$ | NaCl 70 mM, KCl 5 mM, $MgCl_2$ 20 mM, $NaHCO_3$ 10 mM, trehalose 5 mM, HEPES 5 mM, sucrose 115 mM, $Ca^{2+}$ 1 mM, pH 7.2 |
| HL3 high $K^+$ | NaCl 40 mM, KCl 90 mM, $Ca^{2+}$ 1.5 mM, $MgCl_2$ 20 mM, $NaHCO_3$ 10 mM, trehalose 5 mM, HEPES 5 mM, sucrose 5 mM, pH 7.2 |
| 10x PBS | 1.37 M NaCl, 27mM KCl, 100mM $Na_2HPO_4$, 20mM $KH_2PO_4$, pH 7.4 |
| PBSTx | PBS 1x, 0.3% Triton X (v/v) |
| 20xSSC | 20g NaCl, 100.5g Tri-Sodium Citrate, pH 7.0 in 1L |
| TE | 10 mM Tris-HCL, 1mM EDTA, pH 8.0 |

*Table 2.* A list of all the solutions used in the project.

### 2.2.3 smFISH probes

Probes for the smFISH protocol were designed using a protocol described before (Gaspar, Wippich and Ephrussi, 2017). A set of oligonucleotides (28 for the YFP exon) against the gene region of interest was composed using LGC Biosearch Technologies' Stellaris® RNA FISH Probe Designer. The oligonucleotides were pooled and elongated overnight at 37ºC with a ddUTP conjugated to a desired dye (Atto 633 for the YFP probe) using terminal deoxynucleotidyl transferase enzyme from Life Technologies (Thermo Fisher Scientific). The fluorescently labelled oligonucleotides were then purified by Oligo Clean & Concentrator kit (Zymo Research®) and eluted in TE buffer, after which their concentration and degree of labelling were measured using a NanoDrop spectrophotometer. The probes were diluted with TE buffer to 25µM concentration.

### 2.2.4 RNA single molecule *in situ* hybridization (smFISH) on the *Drosophila* larval fillet

RNA single molecule in situ hybridization (smFISH) was carried out as described previously (Titlow *et al.*, 2018). In short, wandering 3$^{rd}$ instar (L3) larvae were dissected in HL3 0.3 mM $Ca^{2+}$ as described before to produce a larval fillet with exposed NMJs (Brent, Werner and McCabe, 2009), fixed for 30 minutes at room temperature (RT) using 4% paraformaldehyde in PBS containing 0/1% Triton-X (PBSTx) and permeabilized 2x for 20 minutes in PBSTx at RT. Samples were then pre-hybridized for 20 minutes at 37ºC in wash buffer (2x SSC, 10% formamide), and then hybridized overnight at 37ºC in hybridization buffer (10% formamide, 10% dextran sulphate, 250nM smFISH probe(s), anti-HRP (**Table 3**) in 2x SSC). Samples were then rinsed in wash buffer again and counterstained with DAPI (1:1000 from 0.5mg/mL stock) in wash buffer for 45min at RT. Next, samples were washed for 45min in wash buffer at RT and incubated in Vectashield anti-fade mounting medium (Vector Laboratories) adjusted for the objective Refractive Index for 30 minutes, and subsequently mounted on the slide in the mounting medium.

### 2.2.5 Immunofluorescence (IF) on the *Drosophila* larval fillet

L3 larvae were dissected and fixed as described in the smFISH protocol. Larvae were then blocked for more than 1h at 4ºC in blocking buffer (PBSTx, 1.0% BSA). Samples were incubated overnight at 4ºC with the primary antibody (**Table 3**) in blocking buffer. The next day, samples were washed for about 1 h and incubated in the secondary antibody solution (conjugated to Alexa Fluor 488, 568 or 647, used at 1:500, from Life Technologies, diluted in PBSTx) together with DAPI (1:1000 from 0.5mg/mL stock) for a further 1h. Samples were then washed for 45min in PBSTx at RT and incubated in Vectashield and mounted as in the smFISH protocol (section 2.2.4).

| Antibody | Detects | Source | Species | Dilution |
|---|---|---|---|---|
| Anti-Dlg1 | Disks large, a post-synaptic scaffolding protein | Developmental Studies Hybridoma Bank, https://dshb.biology.uiowa.edu/ | Mouse | 1:200 |
| Anti-HRP conjugated to Alexa 405, 488, | Neurons | Jackson ImmunoResearch Europe Ltd | Goat | 1:100 |

| | | | | |
|---|---|---|---|---|
| 568 or 647 | | | | |

*Table 3.* A list of all the primary antibodies used in this study.

### 2.2.6 Spaced High $K^+$ depolarization paradigm

The spaced potassium assay has been carried out as described before (Piccioli and Littleton, 2014; Roche *et al.*, 2002; Ataman *et al.*, 2008). Briefly, the larvae were dissected in 0.3 mM $Ca^{2+}$ HL3 and then moved to 1 mM $Ca^{2+}$ HL3. The unstretched larvae were then washed with high $K^+$ HL3 for the periods of 2, 2, 2, 4 and 6 minutes with 15 minutes intervals of 1 mM $Ca^{2+}$ HL3 in between (for RNAi knockdown experiments on *Atpalpha*, *alpha-Cat*, *nrv2*, *shot*, *Nrg*, *Flo-2*, *Vha55*), or periods of 2 minutes, three times, with 10 minutes in between (for RNAi knockdown experiments on *Lac*, *gs2*, *Pdi*). The assay was performed with a minimum of 5 control and 5 RNAi larvae per each experiment and in one replicate for knockdown of *Atpalpha*, *alpha-Cat*, *Vha55*, two replicates for knockdown of *Nrg* and *Flo-2*, six replicates for the knockdown of *Lac*, three replicates for all remaining RNAi knockdown experiments. In each experiment, an internal control was performed at the same time, where the Repo>mCD8-GFP larvae were crossed to UAS-RNAi line against mCherry protein, absent in these larvae, and each experiment was compared to its internal control only. After the spaced potassium pulses, the larvae were then stretched again, left for a period of rest of 30 minutes, and fixed and labelled as described in the IF protocol. For all experiments, segments A2-A5 of muscles 6/7 were imaged.

### 2.2.7 Image acquisition and processing

For the smFISH experiments, the larvae were dissected, fixed and stained with DAPI and anti-HRP antibody conjugated to the DyLight 405 dye, and the anti-YFP exon probe conjugated to Atto-633 dye, as per the smFISH protocol. A minimum of 3 larvae and 15 NMJs were assessed. For the potassium stimulation experiments, a minimum of 5 control and 5 RNAi larvae were dissected, treated as described above (see “Spaced High $K^+$ depolarization paradigm”) fixed and stained with DAPI and anti-HRP antibody conjugated to Alexa-647 dye, and the anti-Dlg1 antibody as described in the IF protocol, and the glial membrane was labelled in endogenously with Repo>mCD8-GFP. Mounted specimens were imaged using an inverted Olympus FV3000 laser scanning confocal microscope or Olympus CSU-W1 SoRa laser spinning disk confocal microscope. Images were acquired using 60x 1.4NA Oil

UPlanSApo objective (FV3000) or 100x 1.51NA Oil UPlanSApo objective, 100x 1.4NA Oil UPlanSApo objective or 60x 1.51NA Oil UPlanSApo objective (SoRa). Laser units were solid state 405, 488, 568 and 640 lasers for both microscopes.

The images were then processed in ImageJ (https://imagej.nih.gov/ij/) (Schneider, Rasband and Eliceiri, 2012). The glial processes at the NMJ are largely flat, hence the 2 dimensional areas of the GFP labelled glial membranes were measured as previously described; these membranes included small sections of non-synaptic motor axon branches from full Z-stack 2D projections as well as glial membrane nearing the synaptic lamella (Brink *et al.*, 2012a). The neurite areas were measured identically, except they were labelled with anti-HRP. The settings used were: the linear auto-contrast, auto-threshold, and area measurement functions of NIH ImageJ (Abràmoff, Magalhães and Ram, 2004). In the spaced potassium stimulation experiment, the ghost boutons were quantified manually.

For statistical analysis, R Studio was used. Each two-dimensional area from each NMJ at muscles constituted an independent replicate ("n") value. The n numbers for each genotype and experiment are specified in respective figure legends. For spaced potassium stimulation experiment, we quantified and reported average log2 foldchange of bouton counts post potassium stimulation compared to RNAi controls and performed the Wilcoxon rank sum test. For the areas' quantification, we calculated foldchange in glial protrusion area, neurite area and their ratio upon knock-down of glial protrusion-localized transcripts. We performed these calculations in two sets: before and after potassium activation assay. For each set, average foldchange for each gene was calculated. Student's t-tests were performed on the data to assess significant differences. The summary statistics are available in Supplementary Table 1 (unstimulated NMJs areas), Supplementary Table 1 (stimulated NMJs areas) and Supplementary Table 3 (stimulated NMJs ghost boutons).

# 3 RESULTS

## 3.1 Collation of multiple studies characterizing transcript localization to peripheral glial cytoplasmic projections

To identify a common set of localized glial transcripts, we performed a meta-analysis of, to our knowledge, all published mammalian localized and synaptic transcriptomic datasets derived from multiple types of glia (Thomsen *et al.*, 2013; Thakurela *et al.*, 2016; Boulay *et al.*, 2017; Sakers *et al.*, 2017; Azevedo *et al.*, 2018; Mazaré *et al.*, 2020; Vasek *et al.*, 2021), outlined in **Table 4.**

| Reference | Cell type | Specimen type | Type of data | Organism |
|---|---|---|---|---|
| Azevedo *et al.*, 2018 | Oligodendrocytes protrusions | Primary cultures of OPCs from rat brain in Boyden Chamber | Soma and protrusion transcriptome | Rat |
| Thomsen *et al.*, 2013 | Perisynaptic astrocytic processes (PAPs) | Type 2 astrocyte mouse cell line C8-S in Boyden Chamber | Soma and protrusion transcriptome | Mouse |
| Thakurela *et al.*, 2016 | Mouse CNS myelin (oligodendrocytes) | Biochemically purified myelin from whole brains of male c57Bl6/N mice | Myelin transcriptome at various developmental stages (P18, P75, 6 and 24 months) | Mouse |
| Boulay *et al.*, 2017 | Astrocyte endfeet | Mechanically isolated brain vessels with attached astrocytic endfeet | Soma and protrusion translatome | Mouse |
| Sakers *et al.*, 2017 | Perisynaptic astrocytic processes (PAPs) | Isolated astrocyte-GFP-tagged ribosome-bound RNA from the synaptoneurosome fraction from homogenized cortices (including hippocampi) | Soma and protrusion transcriptome and translatome | Mouse |
| Castro *et al.*, 2020 | Perisynaptic Schwann Cells | Whole Perisynaptic Schwann Cells FACS sorted from P15-P21 S100β-GFP;NG2-dsRed mice | Whole FACS sorted PSCs | Mouse |
| Mazaré *et al.*, 2020 | Perisynaptic astrocytic processes (PAPs) | Isolated astrocyte-GFP-tagged ribosome-bound RNA from synaptogliosomes from dorsal hippocampi | Soma and protrusion translatome | Mouse |
| Vasek *et al.*, 2021 | Peripheral Microglia Processess (PEMPs) | GFP tagged ribosomes from Peripheral Microglia Processess | Protrusion translatome | Mouse |

*Table 4. A summary of all the available localized and synaptic glial transcriptomic datasets which were analyzed in this study. Most of the datasets explored transcripts localized to glial periphery, but the PSCs dataset was also included although it involved bulk transcriptomics because of its relevance to the glial involvement in synaptic plasticity.*

These glial cell types include four studies of astrocytes, and one study each of oligodendrocytes, micro-dissected myelin and microglia. We also included one bulk transcriptomic study from Perisynaptic Schwann cells (PSCs) that are non-myelinating glia associated with the NMJ that were isolated from mice. We used the PSCs study because the isolated transcripts are associated with synapse activity, and therefore highly relevant in our quest for mechanistic connections between mRNA localization and synaptic plasticity (Castro *et al.*, 2020). The 8 studies used various methods of purifying localized transcripts, which are summarized in Table 4 “Specimen type” column, and in Figure 1A. We collated 8 transcriptomic and 4 TRAP (Translating Ribosome Affinity Purification) datasets, creating a total of 12 analyzable datasets (Figure 1B). For details of how our analysis was performed, see the “Data meta-analysis methods” section of the “Materials and Methods”.

Using our bespoke data processing pipeline, we found 4,801 common transcripts detected in at least 8 libraries of localized mammalian glial transcripts. We tested whether this set of transcripts represents a population of localized mRNAs unique to the periphery of glia or whether they are also shared with the neurite transcriptome. To distinguish these possibilities, we compared the combined list of glial localized transcripts to the group of transcripts shown to commonly localize to the mammalian neuronal projections (von Kügelgen and Chekulaeva, 2020). We found a large overlap between the transcripts present at the periphery of both glia and neurons (Figure 1D). Our observation agrees with recent works highlighting conserved mRNA transport mechanisms between cell types (Goering, Arora and Taliaferro, 2022) and significant overlap of localized transcripts within astrocytes, radial glia and neurons (D'Arcy and Silver, 2020). In contrast, however, transcripts that were translated or preferentially enriched in protrusions displayed limited overlap between neurons and glia, suggesting that cell-type specific regulation of translation or RNA transport could be in place.

### 3.2 Meta-analysis of localized glial transcriptomes yields a predicted group of transcripts localized to the periphery of *Drosophila* peripheral glia

We then asked whether the mammalian glial localized transcripts were likely to be conserved across higher eukaryotes. To address this, we intersected our mammalian dataset with the glial subtypes that extend their processes to the Peripheral Nervous System (PNS) of *Drosophila melanogaster*, which is a highly accessible and well-established model for studying mRNA transport and local translation. We first converted the 4,801 mammalian genes to high confidence *Drosophila* homologues, retaining genes with a DIOPT score of at least 8 as a cutoff (Figure 1C). The conversion produced a list of 3,513 genes that we used to query the glial nuclear transcriptome from the Fly Cell Atlas (Li *et al.*, 2022) (Figure 1E). We chose transcripts that were expressed in perineurial glia (PG) and subperineurial glia (SPG), the glial subtypes known to extend their processes to the *Drosophila* Neuromuscular junction (NMJ) (Figure S1B and S1C). These glia have very long cytoplasmic extensions, and their cell bodies can be hundreds of micrometers away from their furthermost projections (Brink *et al.*, 2012b; Sepp, Schulte and Auld, 2000; Sepp, Schulte and Auld, 2001; Sepp and Auld, 2003) (Figure 1E). We also included ensheathing glia (EG), as they are the closest glial cell type in the Fly Cell Atlas that

corresponds to wrapping glia (WG) of the PNS based on *nrv2* gene expression. The ensheathing glia in the CNS are continuous with the wrapping glia in the PNS, and express similar marker genes (Yildirim *et al.*, 2019) (Figure S1A). Our filtering of the mammalian glial localized mRNAs with high confidence *Drosophila* homologues by expression in any of the three *Drosophila* PNS glial subtypes (PG, SPG and WG/EG) yielded a group of 1700 transcripts that we classify as "predicted to be present" in the projections of the *Drosophila* PNS glia. We hereafter refer to these transcripts as localized.

### 3.3 Gene ontology analysis reveals the enrichment of transcripts related to mRNA trafficking, membrane composition and cytoskeletal regulation

To understand the functional characteristics of this group of localized transcripts, we performed Gene Ontology (GO) analysis followed by semantic similarity clustering of related GO terms (Figure 2). Unclustered individual GO terms are given in Figure S2 and Supplementary Table 2. Our analysis revealed that the localized transcripts were enriched for biological processes involving morphogenesis/development, subcellular localization, cytoskeletal organization, signaling processes, and mRNA metabolism (Figure 2A). In terms of molecular function, RNA-binding, cytoskeleton-binding, as well as transmembrane transporter genes were highly enriched in our gene set (Figure 2B). Finally, our analysis of GO terms for the cellular component showed enrichment of terms related to vesicle/membrane transport, ribonucleoprotein granules and ribosomes in connection with the cytoskeleton, and the synapse, including synaptic terminal, boutons and junctions (Figure 2C). Taken together, our GO enrichment analysis highlights over-representation of functions related to membrane trafficking, cytoskeleton regulation, local translation, and cell-cell communication within the localized transcripts, all of which are likely to be very active at the distal periphery of polarized cells.

### 3.4 The 1700 transcripts predicted to be present at the glial periphery are statistically enriched in neurodegenerative and neuropsychiatric disorders

Neurodegenerative and neuropsychiatric disorders have been associated with disruption of a number of post-transcriptional mechanisms, such as local translation,

RNA-binding protein (RBP) activities and formation of RNA-rich granules (Blanco-Urrejola *et al.*, 2021). To determine whether our predicted *Drosophila* glial peripherally localized transcripts are statistically enriched in associations with previously studied nervous system disorders, we carried out a disease ontology enrichment analysis. We found a significant enrichment of disease terms related to neuropathologies in our set of 1,700 glial protrusion-localized transcripts (Figure 3A). Interestingly, terms related to neurodegeneration and dementia were particularly enriched in the 1,700 genes and were also found in previous studies to be connected to glial related mechanisms that cause the diseases (Blanco-Urrejola *et al.*, 2021). We also compared the set of 1,700 glial protrusion-localized transcripts with the SFARI gene database, which is a well-annotated list of genes that have associations with autism spectrum disorder (https://www.sfari.org/). We found a significant overlap between the 1,700 glial protrusion-localized transcripts and the SFARI genes (Figure 3B), further supporting the idea that mRNA localization in glia and the specific list of 1,700 genes we have highlighted are statistically enriched in genes associated with neurological disorders.

Finally, it was also very interesting to determine whether the 1,700 localized glial transcripts we highlighted are also enriched in signaling and enzymatic pathways. To investigate this possibility, we carried out a reactome-pathway enrichment analysis and found a significant enrichment of terms related to signaling pathways, such as Hedgehog or Wnt pathways, as well as terms related to mRNA translation, mRNA stability regulation and nonsense-mediated decay (Figure 3C). These significant associations highlight the hypothesis that the many of the localized mRNAs at the periphery of glia are required for neuron-glia, glia-muscle or glia-glia communication, and localized mRNA processing and metabolism at the distal cytoplasm of glia. Such mechanisms could potentially include non-canonical mRNA processing that has been previously suggested to be involved in brain physiology and cancer (Pitolli *et al.*, 2022). Moreover, another group that is worth highlighting is the “innate immune system” which is also highly enriched, showing that the availability of gene lists like ours could extend beyond the nervous system context. Analyses like the ones we present here could prove useful in predicting which mRNAs might be localized in immune cells based on whether they are found in neurites.

### 3.5 More than 70% of the previously identified glial transcripts are predicted to be present in the *Drosophila* PNS glia

Do the predicted transcripts indeed localize to the periphery of glial cells? To test our prediction in *Drosophila* glia, we cross-referenced the list of 19 transcripts previously identified experimentally to be present in the *Drosophila* peripheral glia (Titlow *et al.*, 2022) against the list of 1,700 transcripts predicted in this study to be present in the *Drosophila* PNS glia. 15 out of 19 fly genes had high confidence mammalian homologues, so we report our comparison within these 15 genes (see Table 5).

| Found in Titlow et al. | FBgn ID | Is predicted in 1700? |
|---|---|---|
| *Lac* | FBgn0010238 | Yes |
| *Pdi* | FBgn0286818 | Yes |
| *nrv2* | FBgn0015777 | Yes |
| *Lost* | FBgn0263594 | No |
| *Flo-2* | FBgn0264078 | Yes |
| *alpha-Cat* | FBgn0010215 | Yes |
| *Vha55* | FBgn0005671 | Yes |
| *Atpalpha* | FBgn0002921 | Yes |
| *Nrg* | FBgn0264975 | Yes |
| *Cip4* | FBgn0035533 | Yes |
| *Nrx-IV* | FBgn0013997 | No |
| *gs2* | FBgn0001145 | Yes |
| *shot* | FBgn0013733 | Yes |
| *kst* | FBgn0004167 | No |
| *sdk* | FBgn0021764 | No |

*Table 5. A table indicating whether the 19 genes previously predicted to be present in the Drosophila glia have been predicted in the list of 1,700 Drosophila homologs. All transcripts which did not have a high confidence D. melanogaster orthologs of 4,801 genes that were detected in at least 8 datasets (DIOPT score ≥ 8) were removed.*

We found that 11 out of the 15 transcripts (73.33%) were predicted from our analysis of mammalian glial transcripts to localize to the glial periphery in *Drosophila*. As these data originate from a systematic study of the relative distributions of 200 proteins and mRNAs across the larval nervous system (Titlow *et al.*, 2022), we sought to further validate the localization of the 11 genes together with specific glial markers using smFISH (Figure 4 and S4, see “Experimental methods” for details). smFISH showed that indeed all 11 transcripts were present in the peripheral glia at the *Drosophila* NMJ. The single-molecule resolution of mRNA detection also allowed us to characterize the relative levels and distributions of mRNAs more precisely across the motoneuron axons and the surrounding glial protrusions (Figure 4 and

Figure S4). We found specific examples of transcripts that were highly enriched in glia, with much less abundance in the motoneurons, including *gs2*, *nrv2*, *flo-2* and *Lac* (Figure 4 and S4A, B, G respectively). Other transcripts were uniformly distributed in both motoneurons, glia and muscle cells in the NMJ, including *Cip4*, *Pdi*, *Vha55*, *Nrg*, *alpha-Cat*, *Atpalpha*, *shot* (Figure S4, C-F, H-J, respectively). In conclusion, these results show that the localization of transcripts, extrapolated from vertebrates to *Drosophila,* were highly concordant, reliably predicting the presence of multiple mRNAs at the glial periphery and highlighting a possible evolutionary conservation of glial protrusion-localized transcriptome.

### 3.6 Some localized glial transcripts are specifically required functionally in the glia to influence plasticity in the adjacent motoneurons

To expand on our observations further, we tested the potential functional significance of the localized mRNAs at the glial periphery to influence synaptic plasticity of neighboring motoneurons. For this, we aimed to knock-down each transcript in glia, while leaving the motoneurons unaffected in testing for synapse phenotypes. To achieve this goal, we used 13 UAS-RNAi lines (against 11 transcripts) driven by the pan-glial Repo-GAL4 driver (see materials and methods for further details). The impact of modulating the level of each gene in the glia was then assessed in wild type motoneurons by applying the well-established chemical stimulation assay for activity-dependent synaptic plasticity using spaced pulses of potassium (Ataman *et al.*, 2008; Roche *et al.*, 2002; Piccioli and Littleton, 2014; Vasin *et al.*, 2014). We found that 10 of the UAS-RNAi lines were viable until 3$^{rd}$ instar larvae without causing excessive lethality. RNAi knockdown of *Cip4* in glia did not yield viable 3$^{rd}$ instar larvae, so this gene was excluded from our further analysis. Besides the NMJ phenotype, we notably found *Vha55*-RNAi larvae to display smaller brain phenotype (Figure S5), although the overall larvae were otherwise indistinguishable in size from their control counterparts. Therefore, we tested 10 out of 11 localized transcripts in glia for their involvement in regulating synaptic plasticity of motoneurons.

We performed the spaced potassium stimulation assay (Figure 5A) on viable experimental and control larvae (at 3$^{rd}$ instar) and quantified the effect of glial-specific RNAi by counting the number of newly formed neuronal synapse defined as

"ghost" boutons, which are immature synapses that lack post-synaptic density markers like Discs large 1 (*Dlg1*) protein (Ataman *et al.*, 2008; Roche *et al.*, 2002). We found that for 3 of the 10 (*Lac*, *gs2*, *Pdi*) tested transcripts, the RNAi knockdown in the *Drosophila* glia causes a reduction in the number of ghost boutons formed in response to pulses of potassium (Figure 5B, C). We conclude that *Lac*, *gs2* and *Pdi* are required within glia for correct plasticity of motoneuron synapses.

We also assayed the impact on knocking down the localized transcripts in glia on the morphology of the glial projections and of the wild-type axon terminals in the NMJ. We compared the relative morphology of the knocked down glia and wild-type motoneurons in the 3$^{rd}$ instar *Drosophila* larvae without activity stimulation (Figure 5 D, E) or with stimulation (Figure 5 F, G). We found that the knock-down of localized genes resulted in aberrant growth or shrinkage of glial projections as well as the glial to neuron area ratios when compared to control for many of our candidate genes even without stimulation, suggesting a developmental defect. For example, the glial projections in the *shot*-RNAi unstimulated larvae were practically non-existent. While in the control larvae, the glial projections extend on the surface of the muscle cells, in *shot*-RNAi larvae we only observed the sections of non-synaptic motor axon branches covered in glia and no projections on the surface of the muscle (Figure 5D, E). We also saw varying defects in sizes of both glial and neuronal projections after spaced potassium stimulation (Figure 5F, G). Overall, our results show functional significance of many of the localized transcripts and their associated proteins specifically in the glial cells for the correct morphology and function of the *Drosophila* NMJ. 30% of the tested genes are also necessary in glia for the correct synaptic plasticity of the neighboring neuron.

# 4 Discussion

## 4.1 Transcripts localized to the projections of different glial subtypes are required for fine control of the local dynamics

Using meta-analysis of multiple published datasets of peripherally localized mammalian glial mRNAs, we have predicted 1,700 localized transcripts in 3 glial subtypes associated with the *Drosophila* motoneurons and NMJ synapses. These mRNAs are highly enriched in *Drosophila* homologues of human genes with associations in a variety of neurodegenerative and neuropsychiatric diseases, which

also often coincide with molecular and cellular functions that have known associations with the cell periphery (Figure 1). The localized glial mRNA we predict include regulators of cytoskeleton dynamics and remodeling, membrane dynamics, signaling pathways and mRNA metabolism (Figure 2). We at least partly tested the predictions by using smFISH to confirm the localization of 15 out of 19 of the mRNAs that we previously identified as present in *Drosophila* glia (Titlow *et al.*, 2022) and possessing high confidence mammalian homologues. We found that 11 out of the 15 predicted transcripts were localized in the glial periphery near the NMJ, suggesting that our analysis holds strong predictive value (Figure 3). Moreover, by studying the impact of the knock-down of these transcripts specifically in glia, we found that in three cases, they have significant impact on the ability of the adjacent wild-type motoneurons to make new synapses. In other cases, the knock-down of the glial localized transcript causes morphological defects in the motoneuron or the glia themselves (Figure 5). We conclude that our group of 1,700 mRNAs predicted to localize in *Drosophila* glia adjacent to the NMJ are likely to represent a rich resource of functionally interesting transcripts, which in many cases have associations with neurodegenerative, neuropsychiatric and other important nervous system diseases, further emphasizing the power of data interoperability in biological research.

It is important to consider whether the 1,700 transcripts which we predict are localized in the three glial sub-types associated with the NMJ, are in fact a core localized glial transcriptome that is likely localized to the protrusions of any glial cell type. Certainly, the glial sub-types we characterized in *Drosophila* at the NMJ are also present, as defined by specific cell type markers, in association with neurons and synapses in the central brain. Moreover, recent studies suggest that mRNA localization in one cell type mediated by interactions with RBPs can be predictive of the same interactions and localizations in other cell types with very different morphologies and functions (Goering, Arora and Taliaferro, 2022). It has also been shown that radial glia, astrocytes, and neurons, all of which have quite distinct morphologies and functions, share a significant overlap in the types of mRNAs localized to their protrusions (D'Arcy and Silver, 2020). Perhaps cytoplasmic peripheries of any kind of cell type have many properties in common, such as membrane trafficking and cytoskeletal dynamics, all of which require similar core fine

local regulation by mRNA localization, regardless of the details of the specific cell type and its functions.

### 4.2 Glial protrusion transcriptomes contain a significant enrichment of disease ontology terms related to neuropathologies

Our analysis has indicated a significant enrichment of terms related to associations with nervous system diseases among the 1,700 *Drosophila* homologues with predicted glial mRNA localization (Figure 3). Moreover, this group of genes has a statistically significant overlap with the SFARI database, which contains a list of genes implicated in autism spectrum disorder (ASD). There is a growing interest in the role that glial cells may play in the mechanistic causes of diverse diseases related to nervous system development and function. Indeed, it has been suggested that mRNA localization and local translation could cause glial-induced pathological effects (Sloan and Barres, 2013; Prater, Latimer and Jayadev, 2022). Our results bolster the idea that glial cells may play more important roles than previously appreciated in the causes of these diseases. The dearth of literature in this area only serves to emphasize the need for more experimental work with a holistic approach to the nervous system, including glia and their communication with neurons at tripartite synapses. Although aggregated research made available in databases like SFARI mostly focuses on neuronal studies, our work shows that many SFARI genes are transcribed into mRNA that is localized to glial protrusions. We have also shown that the reactome-pathway analysis of glial localized transcripts uncovered many enriched terms related both to signaling and mRNA metabolism, providing hints at potential unexplored mechanisms related with some of these nervous system disorders.

An important direction of future research will be to characterize local translation at the peripheral cytoplasm of glia in response to signaling and neuronal activity, as was done in one recent study, which we included in our meta-analysis (Mazaré *et al.*, 2020). The *Drosophila* larval system is a particularly good experimental system to study glia in relation to plasticity, because of the ease of access to the NMJ and the ability to manipulate the plasticity of the motoneurons. The spaced potassium stimulation assay, electrophysiology or optogenetics all allow the easy observation of

the neuron-glia interplay in response to neuronal activity. Moreover, the extensive genetic toolbox available in *Drosophila* makes the model very tractable and well suited to studying the mechanistic effects of the introduction of disease alleles into synaptic glia.

### 4.3 Vertebrate localization data meta-analysis correctly predicts mRNA localization for the majority of transcripts

Using smFISH we confirmed, with greater precision, the presence of 11 transcripts of interest in *Drosophila* glial projections, which we had discovered in a recent survey of 200 transcripts across the larval nervous system (Titlow *et al.*, 2022). We have focused on the glial cell subtypes that reach the *Drosophila* NMJ because of their extensive morphologies and close contacts with the NMJ synapses (Figure S1). The NMJ associated glial subtypes are also present in the central brain, but unlike in the larval brain, in the NMJ the individual glial projections can be observed under the microscope together with individual synapses. Building on our prior work (Titlow *et al.*, 2022), we confirmed that the mammalian localization data, which we re-analysed and intersected with *Drosophila* glia, correctly predicts glial mRNA localization in *Drosophila*. We conclude that peripheral glial mRNA localization is a common and conserved phenomenon and propose that it is therefore likely to be functionally important. Naturally our work is limited by the number of transcripts that could be tested. In the future, it will be important to continue to explore the localization of many more of the 1,700 *Drosophila* transcripts and test their functional requirement in glia as well as their potential implications for novel mechanisms of diseases of the nervous system.

## 5 Contributions, conflict of interest, funding details

### Author contributions:

**Dalia S. Gala:** Conceptualization, Methodology, Validation, Formal analysis, Investigation, Data Curation, Writing - Original Draft, Writing - Review & Editing, Visualization. **Jeffrey Y. Lee:** Conceptualization, Methodology, Software, Validation, Formal analysis, Resources, Data Curation, Writing - Review & Editing,

Visualization. **Maria Kiourlappou:** Methodology, Software, Formal analysis, Data Curation, Writing - Review & Editing. **Joshua S. Titlow:** Conceptualization, Methodology, Writing - Review & Editing, Supervision. **Rita O. Teodoro**: Methodology, Resources, Writing - Review & Editing, Supervision. **Ilan Davis:** Conceptualization, Resources, Writing - Original Draft, Writing - Review & Editing, Supervision, Project administration, Funding acquisition.

### Conflicts of Interest:

The authors declare no competing or financial interests.

### Funding statement:

This work was funded by a Wellcome Investigator Award 209412/Z/17/Z and Wellcome Strategic Awards (Micron Oxford) 091911/B/10/Z and 107457/Z/15/Z to I.D. M.K. was supported by the Biotechnology and Biosciences Research Council (BBSRC), grant numbers: (BB/M011224/1) and (BB/S507623/1). D.S.G. is funded by Medial Sciences Graduate Studentships, University of Oxford. R.O.T. is funded by iNOVA4Health – UIDB/04462/2020 and EXPL/BIA-CEL/1484/2021.

## 6 References

Abràmoff, M. D., Magalhães, P. J. and Ram, S. J. (2004) 'Image processing with ImageJ', *Biophotonics international,* 11(7), pp. 36-42.

Alexa, A. and Rahnenfuhrer, J. 2022. *topGO: Enrichment Analysis for Gene Ontology*. R package version 2.48.0. ed.

Allen, N. J. and Lyons, D. A. (2018) 'Glia as architects of central nervous system formation and function', *Science,* 362(6411), pp. 181-185.

Andoh, M. and Koyama, R. (2021) 'Microglia regulate synaptic development and plasticity', *Developmental Neurobiology,* 81(5), pp. 568-590.

Ataman, B., Ashley, J., Gorczyca, M., Ramachandran, P., Fouquet, W., Sigrist, S. J. and Budnik, V. (2008) 'Rapid Activity-Dependent Modifications in Synaptic Structure and Function Require Bidirectional Wnt Signaling', *Neuron*.

Azevedo, M. M., Domingues, H. S., Cordelières, F. P., Sampaio, P., Seixas, A. I. and Relvas, J. B. (2018) 'Jmy regulates oligodendrocyte differentiation via modulation of actin cytoskeleton dynamics', *GLIA*.

Bacmeister, C. M., Barr, H. J., McClain, C. R., Thornton, M. A., Nettles, D., Welle, C. G. and Hughes, E. G. (2020) 'Motor learning promotes remyelination via new and surviving oligodendrocytes', *Nat Neurosci,* 23(7), pp. 819-831.

Biever, A., Donlin-Asp, P. G. and Schuman, E. M. (2019) 'Local translation in neuronal processes', *Current Opinion in Neurobiology,* 57, pp. 141-148.

Blanco-Urrejola, M., Gaminde-Blasco, A., Gamarra, M., de la Cruz, A., Vecino, E., Alberdi, E. and Baleriola, J. (2021) 'RNA Localization and Local Translation in Glia in Neurological and Neurodegenerative Diseases: Lessons from Neurons', *Cells*.

Boulay, A. C., Saubameá, B., Adam, N., Chasseigneaux, S., Mazaré, N., Gilbert, A., Bahin, M., Bastianelli, L., Blugeon, C., Perrin, S., Pouch, J., Ducos, B., Le Crom, S., Genovesio, A., Chrétien, F., Declèves, X., Laplanche, J. L. and Cohen-Salmon, M. (2017) 'Translation in astrocyte distal processes sets molecular heterogeneity at the gliovascular interface', *Cell Discovery,* 3.

Bray, N. L., Pimentel, H., Melsted, P. and Pachter, L. (2016) 'Near-optimal probabilistic RNA-seq quantification', *Nature Biotechnology,* 34(5), pp. 525-527.

Brink, D. L., Gilbert, M., Xie, X., Petley-Ragan, L. and Auld, V. J. (2012a) 'Glial processes at the Drosophila larval neuromuscular junction match synaptic growth', *PLoS One,* 7(5), pp. e37876.

Brink, D. L., Gilbert, M., Xie, X., Petley-Ragan, L. and Auld, V. J. (2012b) 'Glial processes at the Drosophila larval neuromuscular junction match synaptic growth', *PLoS ONE*.

Bushnell, B., Rood, J. and Singer, E. (2017) 'BBMerge – Accurate paired shotgun read merging via overlap', *PLOS ONE,* 12(10), pp. e0185056.

Castro, R., Taetzsch, T., Vaughan, S. K., Godbe, K., Chappell, J., Settlage, R. E. and Valdez, G. (2020) 'Specific labeling of synaptic schwann cells reveals unique cellular and molecular features', *eLife*.

D'Arcy, B. R. and Silver, D. L. (2020) 'Local gene regulation in radial glia: Lessons from across the nervous system', *Traffic,* 21(12), pp. 737-748.

Daniel E Shumer, N. J. N. N. P. S. (2017) '乳鼠心肌提取 HHS Public Access', *Physiology & behavior,* 176(12), pp. 139-148.

de Faria, O., Pivonkova, H., Varga, B., Timmler, S., Evans, K. A. and Káradóttir, R. T. (2021) 'Periods of synchronized myelin changes shape brain function and plasticity', *Nat Neurosci,* 24(11), pp. 1508-1521.

De Pittà, M., Brunel, N. and Volterra, A. (2016) 'Astrocytes: Orchestrating synaptic plasticity?', *Neuroscience,* 323, pp. 43-61.

Fields, R. D. (2005) 'Myelination: An overlooked mechanism of synaptic plasticity?', *Neuroscientist,* 11(6), pp. 528-531.

Fields, R. D. (2008) 'Oligodendrocytes changing the rules: action potentials in glia and oligodendrocytes controlling action potentials', *Neuroscientist,* 14(6), pp. 540-3.

Fields, R. D. and Bukalo, O. (2020) 'Myelin makes memories', *Nat Neurosci,* 23(4), pp. 469-470.

Goering, R., Arora, A. and Taliaferro, J. M. (2022) 'RNA localization mechanisms transcend cell morphology', *bioRxiv*, pp. 2022.04.14.488401.

Graeber, M. B. (2010) 'Changing face of microglia', *Science,* 330(6005), pp. 783-8.

Gu, Z. and Hübschmann, D. (2022) 'Simplify enrichment: A bioconductor package for clustering and visualizing functional enrichment results', *Genomics Proteomics Bioinformatics*.

Holt, C. E., Martin, K. C. and Schuman, E. M. (2019) 'Local translation in neurons: visualization and function', *Nature Structural and Molecular Biology,* 26(7), pp. 557-566.

Hu, Y., Flockhart, I., Vinayagam, A., Bergwitz, C., Berger, B., Perrimon, N. and Mohr, S. E. (2011) 'An integrative approach to ortholog prediction for disease-focused and other functional studies', *BMC Bioinformatics,* 12, pp. 357.

Ignatiadis, N., Klaus, B., Zaugg, J. B. and Huber, W. (2016) 'Data-driven hypothesis weighting increases detection power in genome-scale multiple testing', *Nature Methods,* 13(7), pp. 577-580.

Jessen, K. R., Mirsky, R. and Lloyd, A. C. (2015) 'Schwann cells: Development and role in nerve repair', *Cold Spring Harbor Perspectives in Biology,* 7(7), pp. 1-15.

Li, H. and Janssens, J. and De Waegeneer, M. and Kolluru, S. S. and Davie, K. and Gardeux, V. and Saelens, W. and David, F. P. A. and Brbić, M. and Spanier, K. and Leskovec, J. and McLaughlin, C. N. and Xie, Q. and Jones, R. C. and Brueckner, K. and Shim, J. and Tattikota, S. G. and Schnorrer, F. and Rust, K. and Nystul, T. G. and Carvalho-Santos, Z. and Ribeiro, C. and Pal, S. and Mahadevaraju, S. and Przytycka, T. M. and Allen, A. M. and Goodwin, S. F. and Berry, C. W. and Fuller, M. T. and White-Cooper, H. and Matunis, E. L. and DiNardo, S. and Galenza, A. and O'Brien, L. E. and Dow, J. A. T. and Jasper, H. and Oliver, B. and Perrimon, N. and Deplancke, B. and Quake, S. R. and Luo, L. and Aerts, S. and Agarwal, D. and Ahmed-Braimah, Y. and Arbeitman, M. and Ariss, M. M. and Augsburger, J. and Ayush, K. and Baker, C. C. and Banisch, T. and Birker, K. and Bodmer, R. and Bolival, B. and Brantley, S. E. and Brill, J. A. and Brown, N. C. and Buehner, N. A. and Cai, X. T. and Cardoso-Figueiredo, R. and Casares, F. and Chang, A. and Clandinin, T. R. and Crasta, S. and Desplan, C. and Detweiler, A. M. and Dhakan, D. B. and Donà, E. and Engert, S. and Floc'hlay, S. and George, N. and González-Segarra, A. J. and Groves, A. K. and Gumbin, S. and Guo, Y. and Harris, D. E. and Heifetz, Y. and Holtz, S. L. and Horns, F. and Hudry, B. and Hung, R. J. and Jan, Y. N. and Jaszczak, J. S. and Jefferis, G. S. X. E. and Karkanias, J. and Karr, T. L. and Katheder, N. S. and Kezos, J. and Kim, A. A. and Kim, S. K. and Kockel, L. and Konstantinides, N. and Kornberg, T. B. and Krause, H. M. and Labott, A. T. and Laturney, M. and Lehmann, R. and Leinwand, S. and Li, J. and Li, J. S. S. and Li, K. and Li, L. and Li, T. and Litovchenko, M. and Liu, H. H. and Liu, Y. and Lu, T. C. and Manning, J. and Mase, A. and Matera-Vatnick, M. and Matias, N. R. and McDonough-Goldstein, C. E. and McGeever, A. and McLachlan, A. D. and Moreno-Roman, P. and Neff, N. and Neville, M. and Ngo, S. and Nielsen, T. and O'Brien, C. E. and Osumi-Sutherland, D. and Özel, M. N. and Papatheodorou, I. and Petkovic, M. and Pilgrim, C. and Pisco, A. O. and Reisenman, C. and Sanders, E. N. and Dos Santos, G. and Scott, K. and Sherlekar, A. and Shiu, P. and Sims, D. and Sit, R. V. and Slaidina, M. and Smith, H. E. and Sterne, G. and Su, Y. H. and Sutton, D. and Tamayo, M. and Tan, M. and Tastekin, I. and Treiber, C. and Vacek, D. and Vogler, G. and Waddell, S. and Wang, W. and Wilson, R. I. and Wolfner, M. F. and Wong, Y. E. and Xie, A. and Xu, J. and Yamamoto, S. and Yan, J. and Yao, Z. and Yoda, K. and Zhu, R. and Zinzen, R. P. and Consortium§, F. (2022) 'Fly Cell Atlas: A single-nucleus transcriptomic atlas of the adult fruit fly', *Science,* 375(6584), pp. eabk2432.

Love, M. I., Huber, W. and Anders, S. (2014) 'Moderated estimation of fold change and dispersion for RNA-seq data with DESeq2', *Genome Biology,* 15(12), pp. 550.

Mazaré, N., Oudart, M., Moulard, J., Cheung, G., Tortuyaux, R., Mailly, P., Mazaud, D., Bemelmans, A. P., Boulay, A. C., Blugeon, C., Jourdren, L., Le Crom, S., Rouach, N. and Cohen-Salmon, M. (2020) 'Local Translation in Perisynaptic Astrocytic Processes Is Specific and Changes after Fear Conditioning', *Cell Reports*.

Melsted, P., Booeshaghi, A. S., Liu, L., Gao, F., Lu, L., Min, K. H., da Veiga Beltrame, E., Hjörleifsson, K. E., Gehring, J. and Pachter, L. (2021) 'Modular, efficient and constant-memory single-cell RNA-seq preprocessing', *Nature Biotechnology,* 39(7), pp. 813-818.

Meservey, L. M., Topkar, V. V. and Fu, M. m. (2021) 'mRNA Transport and Local Translation in Glia', *Trends in Cell Biology,* 31(6), pp. 419-423.

Morris, G. P., Clark, I. A., Zinn, R. and Vissel, B. (2013) 'Microglia: A new frontier for synaptic plasticity, learning and memory, and neurodegenerative disease research', *Neurobiology of Learning and Memory,* 105, pp. 40-53.

Ota, Y., Zanetti, A. T. and Hallock, R. M. (2013) 'The role of astrocytes in the regulation of synaptic plasticity and memory formation', *Neural Plast,* 2013, pp. 185463.

Pan, S., Mayoral, S. R., Choi, H. S., Chan, J. R. and Kheirbek, M. A. (2020) 'Preservation of a remote fear memory requires new myelin formation', *Nat Neurosci,* 23(4), pp. 487-499.

Piccioli, Z. D. and Littleton, J. T. (2014) 'Retrograde BMP signaling modulates rapid activity-dependent synaptic growth via presynaptic LIM kinase regulation of cofilin', *J Neurosci,* 34(12), pp. 4371-81.

Pitolli, C., Marini, A., Sette, C. and Pagliarini, V. (2022) 'Non-Canonical Splicing and Its Implications in Brain Physiology and Cancer', *Int J Mol Sci,* 23(5).

Prater, K. E., Latimer, C. S. and Jayadev, S. (2022) 'Glial TDP-43 and TDP-43 induced glial pathology, focus on neurodegenerative proteinopathy syndromes', *Glia,* 70(2), pp. 239-255.

Rangaraju, V., tom Dieck, S. and Schuman, E. M. (2017) 'Local translation in neuronal compartments: how local is local?', *EMBO reports,* 18(5), pp. 693-711.

Ransom, B. R. and Ransom, C. B. (2012) *Astrocytes: Multitalented stars of the central nervous system.*

Roche, J. P., Packard, M. C., Moeckel-Cole, S. and Budnik, V. (2002) 'Regulation of synaptic plasticity and synaptic vesicle dynamics by the PDZ protein scribble', *Journal of Neuroscience*.

Sakers, K., Lake, A. M., Khazanchi, R., Ouwenga, R., Vasek, M. J., Dani, A. and Dougherty, J. D. (2017) 'Astrocytes locally translate transcripts in their peripheral processes', *Proceedings of the National Academy of Sciences of the United States of America,* 114(19), pp. E3830-E3838.

Schafer, D. P., Lehrman, E. K., Kautzman, A. G., Koyama, R., Mardinly, A. R., Yamasaki, R., Ransohoff, R. M., Greenberg, M. E., Barres, B. A. and Stevens, B. (2012) 'Microglia sculpt postnatal neural circuits in an activity and complement-dependent manner', *Neuron,* 74(4), pp. 691-705.

Schneider, C. A., Rasband, W. S. and Eliceiri, K. W. (2012) 'NIH Image to ImageJ: 25 years of image analysis', *Nat Methods,* 9(7), pp. 671-5.

Sepp, K. J. and Auld, V. J. (2003) 'Reciprocal Interactions between Neurons and Glia Are Required for', *Cell,* 23(23), pp. 8221-8230.

Sepp, K. J., Schulte, J. and Auld, V. J. (2000) 'Developmental dynamics of peripheral glia in Drosophila melanogaster', *Glia,* 30(2), pp. 122-133.

Sepp, K. J., Schulte, J. and Auld, V. J. (2001) 'Peripheral glia direct axon guidance across the CNS/PNS transition zone', *Developmental Biology,* 238(1), pp. 47-63.

Sloan, S. A. and Barres, B. A. (2013) 'Glia as primary drivers of neuropathology in TDP-43 proteinopathies', *Proc Natl Acad Sci U S A,* 110(12), pp. 4439-40.

Smith, W. B., Aakalu, G. and Schuman, E. M. (2001) 'Local protein synthesis in neurons Girish Aakalu and', *Current Biology*, pp. 901-903.

Sutton, M. A. and Schuman, E. M. (2006) 'Dendritic Protein Synthesis, Synaptic Plasticity, and Memory', *Cell,* 127(1), pp. 49-58.

Terenzio, M., Schiavo, G. and Fainzilber, M. (2017) 'Compartmentalized Signaling in Neurons: From Cell Biology to Neuroscience', *Neuron,* 96(3), pp. 667-679.

Thakurela, S., Garding, A., Jung, R. B., Müller, C., Goebbels, S., White, R., Werner, H. B. and Tiwari, V. K. (2016) 'The transcriptome of mouse central nervous system myelin', *Scientific Reports*.

Thomsen, R., Pallesen, J., Daugaard, T. F., Børglum, A. D. and Nielsen, A. L. (2013) 'Genome wide assessment of mRNA in astrocyte protrusions by direct RNA sequencing reveals mRNA localization for the intermediate filament protein nestin', *Glia,* 61(11), pp. 1922-1937.

Titlow, J. S., Kiourlappou, M., Palanca, A., Lee, J. Y., Gala, D. S., Ennis, D., Yu, J. J. S., Young, F. L., Susano Pinto, D. M., Garforth, S., Francis, H. S., Strivens, F., Mulvey, H., Dallman-Porter, A., Thornton, S., Arman, D., Järvelin, A. I., Thompson, M. K., Kounatidis, I., Parton, R. M., Taylor, S. and Davis, I. (2022) 'Systematic analysis of YFP gene traps reveals common discordance between mRNA and protein across the nervous system', *bioRxiv*, pp. 2022.03.21.485142.

Vasek, M. J., Deajon-jackson, J. D., Liu, Y., Crosby, H. W. and Mo, S. L. (2021) 'Microglia perform local protein synthesis at perisynaptic and phagocytic structures Affiliations : Department of Genetics , Washington University School of Medicine , 660 S . Euclid Ave , Department of Psychiatry , Washington University School of Medicine'.

Vasin, A., Zueva, L., Torrez, C., Volfson, D., Littleton, J. T. and Bykhovskaia, M. (2014) 'Synapsin regulates activity-dependent outgrowth of synaptic boutons at the Drosophila neuromuscular junction', *J Neurosci,* 34(32), pp. 10554-63.

Volterra, A. and Meldolesi, J. (2005) 'Astrocytes, from brain glue to communication elements: the revolution continues', *Nature Reviews Neuroscience,* 6(8), pp. 626-640.

von Kügelgen, N. and Chekulaeva, M. 2020. Conservation of a core neurite transcriptome across neuronal types and species.

Wang, D. O., Martin, K. C. and Zukin, R. S. (2010) 'Spatially restricting gene expression by local translation at synapses', *Trends in Neurosciences,* 33(4), pp. 173-182.

Wang, Y., Fu, A. K. Y. and Ip, N. Y. (2022) 'Instructive roles of astrocytes in hippocampal synaptic plasticity: neuronal activity-dependent regulatory mechanisms', *FEBS J,* 289(8), pp. 2202-2218.

Xie, X. and Auld, V. J. (2011) 'Integrins are necessary for the development and maintenance of the glial layers in the Drosophila peripheral nerve', *Development,* 138(17), pp. 3813-22.

Yildirim, K., Petri, J., Kottmeier, R. and Klämbt, C. (2019) 'Drosophila glia: Few cell types and many conserved functions', *Glia,* 67(1), pp. 5-26.

# 7 Figure legends

**Figure 1. Conserved transcripts localized to glial protrusions.** A) A graphical representation of the techniques used to separate the protrusion-localized transcripts in each study, with the exception of PSCs (middle), where whole cells were used. B) Bar graph showing the datasets included in this study. High confidence expression cut-off was set at TPM > 10, and transcripts detected in more than 3 independent datasets are shown in orange color. C) Identification of high confidence *D. melanogaster* orthologs of 4,801 genes that were detected in at least 8 datasets. DRSC Integrative Ortholog Prediction Tool (DIOPT) score of 8 was used as cut-off. D) Comparison of transcripts localized, enriched or translated in the glial protrusion and/or neurites (von Kügelgen and Chekulaeva, 2020). Transcripts were considered enriched when log2FoldChange > 0 and adjusted p-value < 0.05, comparing protrusion and soma compartment-specific RNA-seq libraries. TRAP-seq TPM > 10 was considered as existence of translation. E) t-SNE plot of combined glial single-nuclei RNA-seq from the Fly Cell Atlas (Li *et al.*, 2022). Perineurial, subperineurial and ensheathing glial cell clusters are depicted in orange-red colors. F) A schematic representing the distribution and location of glial cells in the *Drosophila* 3$^{rd}$ instar larva. Six subtypes of glia exist in the larvae: perineurial and subperineurial glia, cortex glia, astrocyte-like and ensheathing glial cells and, finally, the peripheral nervous system (PNS) specific wrapping glia (Yildirim *et al.*, 2019). Ensheathing glia of the CNS are continuous with the wrapping glia of the CNS. The perineurial and subperineurial glia have long and extensive projections which reach all the way to the neuromuscular junction (NMJ).

**Figure S1. Confocal images of *Drosophila* peripheral glia.** Confocal images representing the location of **A)** wrapping glia (*nrv2*-GAL4), **B)** subperineurial glia (Mdr65-GAL4) and **C)** perineurial glia (46F-GAL4) in the *Drosophila* 3rd instar larva. All three of these glial subtypes produce extensive projections which reach hundreds of microns away from the cell body and reach the neuromuscular junction (NMJ) (middle two panels of each section). These three glial cell subtypes were chosen in our filtering for their elongated morphologies and the direct microscopically observable contact with the NMJ synapse. For each of A), B) and C): **i)** represents the 10x overview of the whole dissected larva, **ii)** represents a 40x zoom of segments A2 and A3 of muscles 6/7. **iii)** presents an overview of the NMJ, and **iv)** is a zoomed-in section of each of the images in **iii)**, as indicated by the white boxes. **v)** and **vi)** show the individual channels from **iv)** for clarity, with the channel label specified in the top left corner of **v)** - glia and **vi)** – anti-HRP.

**Figure 2 Functional annotation of glial protrusion-localized transcripts. A-C)** Overviews of gene ontology (GO) terms enriched in the 1,700 glial protrusion-localized transcripts Biological Process, Molecular Function and Cellular Component categories. Enriched GO terms (FoldChange > 1.5, adjusted p-value < 0.01) were clustered based on the semantic similarity. Word clouds for each cluster showover-represented terms. *D. melanogaster* genes with high-confidence orthologues to *M. musculus* genes (DIOPT score $\geq 8$) were used as background.

**Figure S2. Enriched gene ontology (GO) terms of glial protrusion-localized transcripts. A-C)** Volcano plot of GO terms enriched in the 1,700 glial protrusion-localized transcripts in Biological Process, Molecular Function and Cellular Component categories. *D. melanogaster* genes with high-confidence orthologues to *M. musculus* genes (DIOPT score ≥ 8) were used as background. Full GO enrichment analysis table is given in Supplementary Table 2.

**Figure 3. Association of glial protrusion-localized transcripts with disease. A)** Enrichment of disease ontology (DO) terms in the 1,700 glial protrusion-localized transcripts. DO terms from *D. melanogaster* genes with high-confidence orthologues

to *M. musculus* genes (DIOPT score ≥ 8) were used as background. Enrichment was assessed with hypergeometric test and corrected for multiple hypothesis testing. **B)** Significant overlap between the 1,700 glial protrusion-localized transcripts and the SFARI list of genes. SFARI gene is an annotated list of genes that have been investigated in the context of autism spectrum disorder. 1,095 *H. sapiens* SFARI genes were converted to *D. melanogaster* genes (DIOPT score ≥ 8) before the statistical enrichment. **C)** Reactome pathway enrichment analysis of the 1,700 glial protrusion-localized transcripts against the whole D. Melanogaster genome as background. The size of the of the points shows the number of localized genes corresponding to the term and the color of the point indicates the parent term in the Reactome pathways hierarchy. Enrichment was assessed with hypergeometric test and corrected for multiple hypothesis testing.

**Figure 4. Localization of *gs2*::YFP transcripts in *Drosophila* glia. A)** A confocal image of the *Drosophila* 3$^{rd}$ instar larva NMJ (Segment A4), showing the neuron and muscle cell nuclei in blue (anti-HRP antibody conjugated to Alexa-405 fluor and DAPI, respectively), *gs2*::YFP protein in green, glial membrane of perisynaptic glia labelled with Repo>mCD8-mCherry in magenta, and the YFP exon associated with *gs2*::YFP protein in white (Atto-633). **B-D)** A single-channel view (see label) of a zoomed-in area **i)** of A) in which multiple mRNA molecules are present in the glial projection. **E)** A zoomed in area **ii)** of A) showing the entire length of the perisynaptic glia at that synapse with the mRNA molecules distributed regularly throughout the glial cell projections.

**Figure S4. Localization of predicted transcripts in *Drosophila* glia. B-K)** Confocal images of the *Drosophila* 3$^{rd}$ instar larva NMJs (Segments A3 or A4), showing the **i)** neuron and muscle cell nuclei in blue (anti-HRP antibody conjugated to Alexa-405 fluor and DAPI, respectively), YFP conjugated proteins in green (see in-image label for details), glial membrane of perisynaptic glia labelled with Repo>mCD8-mCherry in magenta, and the YFP exon associated with the protein in white (Atto-633). For all transcripts, mRNA was detected within glial membrane

labelling, as indicated in **ii)** for each panel, where a zoomed in area denoted by a white rectangle in i) is presented.

**Figure 5. Knockdown of glial localized transcripts has functional significance.** **A)** A schematic representation of the spaced potassium stimulation assay used in this study. Larvae are dissected and subjected to pulses of high potassium solution mimicking neuromuscular stimulation. After the assay has been completed, newly formed axon terminal endings with immature synapses, called “ghost boutons”, can be detected using anti-HRP antibody labelling thanks to the lack of the post-synaptic density present, which can be labelled using anti-Discs-large antibody, which the ghost boutons lack. **B)** Knock-downs of multiple glial protrusion-localized transcripts disrupt synaptic plasticity. Bar graph represents average log2 FoldChange of bouton counts post potassium stimulation compared to RNAi Controls. Statistically significant changes are highlighted in orange color. Wilcoxon rank sum test p-values are reported. N = 30(*alpha-Cat*-RNAi), 30(*Atpalpha*-RNAi), 58(*Flo-2*-RNAi), 28(*Vha55*-RNAi), 98(*gs2*-RNAi), 238(*Lac*-RNAi), 48(*Nrg*-RNAi), 73(*nrv2*-RNAi), 114(*Pdi*-RNAi), 76(*shot*-RNAi) NMJs) **C)** Confocal images showing representative control **(i-iii)** and *gs2*-RNAi **(iv-vi)** synapses from the spaced potassium assay experiment. Axon terminal and ghost boutons are labelled in green, and the anti-Discs-large antibody labelling in magenta in i) and iv). ii) and iii) represent the area inside the white rectangle in i) (see in-image labels for details). v) and vi) represent the area inside the white rectangle in iv). ii) and iii) show multiple ghost boutons lacking the post-synaptic density for the Control panel indicated with orange asterisks. v) and vi) show an extreme case where no ghost boutons were found for that NMJ is presented for the *gs2*-RNAi panel. **D)** Confocal images showing representative control (i-iii) and *shot*-RNAi (iv-vi) synapses (see in-image labels for details). NMJ glial projections for *shot*-RNAi (iv) are much less expansive than the control in the unstimulated NMJs (i). **E)** Confocal images showing representative control (i) and *Pdi*-RNAi (ii) synapses (see in-image labels for details). The NMJ areas are much smaller for the *Pdi*-RNAi NMJs when compared to the control in the stimulated NMJs. **F-G)** Foldchange in glial protrusion area, neurite area and their ratio upon knock-down of glial protrusion-localized transcripts before (F, N = 28(*alpha-Cat*-RNAi), 30(*Atpalpha*-RNAi), 30(*Flo-2*-RNAi), 23(*Vha55*-RNAi), 30(*gs2*-

RNAi), 28(*Lac*-RNAi), 23(*Nrg*-RNAi), 28(*nrv2*-RNAi), 28(*Pdi*-RNAi), 27(*shot*-RNAi) NMJs)) and after (G, N = 30(*alpha-Cat*-RNAi), 30(*Atpalpha*-RNAi), 58(*Flo-2*-RNAi), 28(*Vha55*-RNAi), 97(*gs2*-RNAi), 239(*Lac*-RNAi), 48(*Nrg*-RNAi), 73(*nrv2*-RNAi), 114(*Pdi*-RNAi), 79(*shot*-RNAi) NMJs)) potassium activation assay. Data represents average foldchange for each gene. Student's t-test.

**Figure S5. Knockdown of *Vha55* causes a small larval brain phenotype.** Confocal images showing the marked difference in size between the A) control (Repo-GAL4>UAS-mCD8-GFP; UAS-*mCherry*-RNAi) and B) *Vha55*-RNAi (Repo-GAL4>UAS-mCD8-GFP;UAS-*Vha55*-RNAi) brains for 3$^{rd}$ instar larvae of very similar sizes.

# Figure 1



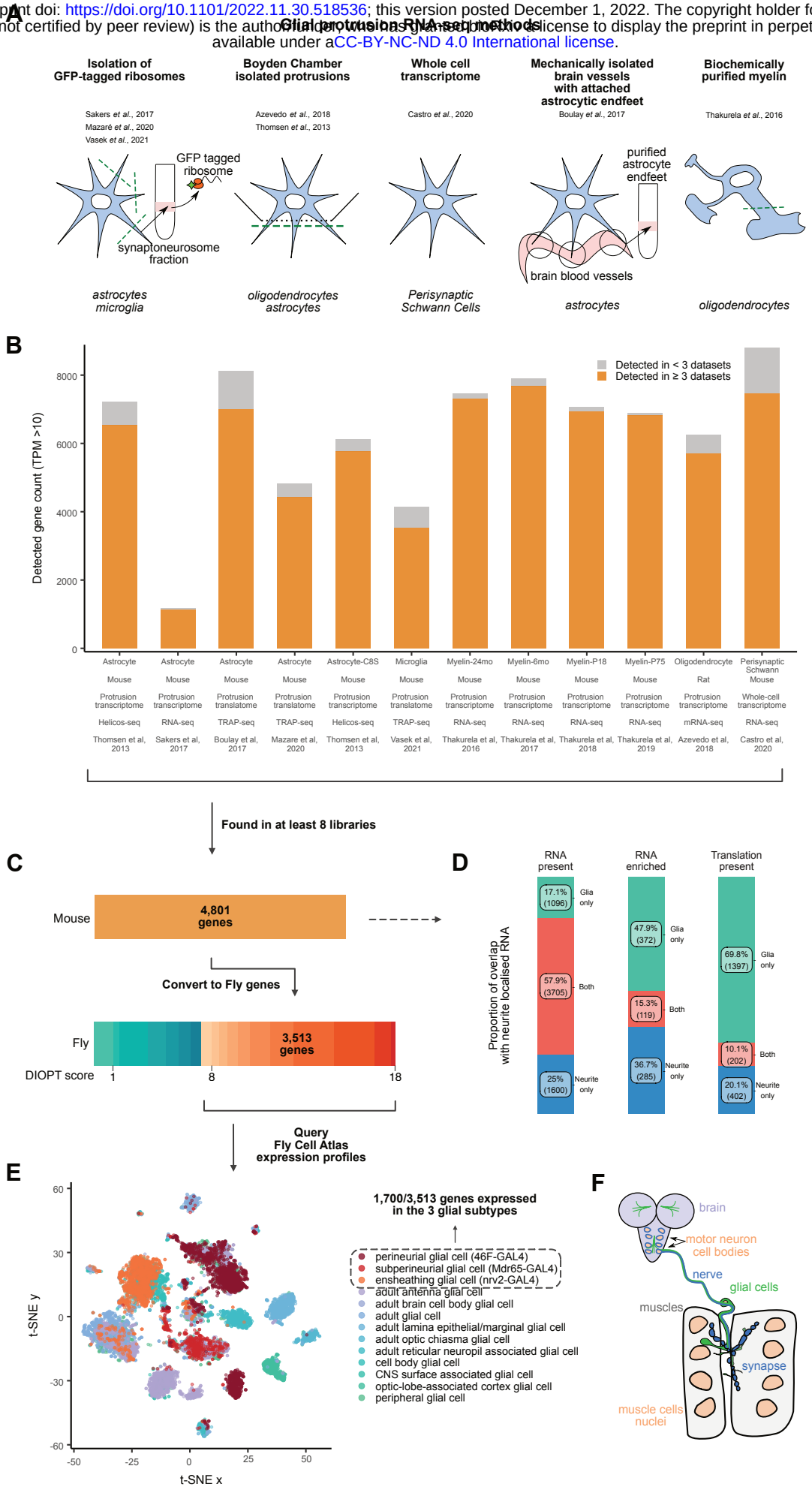

# Figure S1



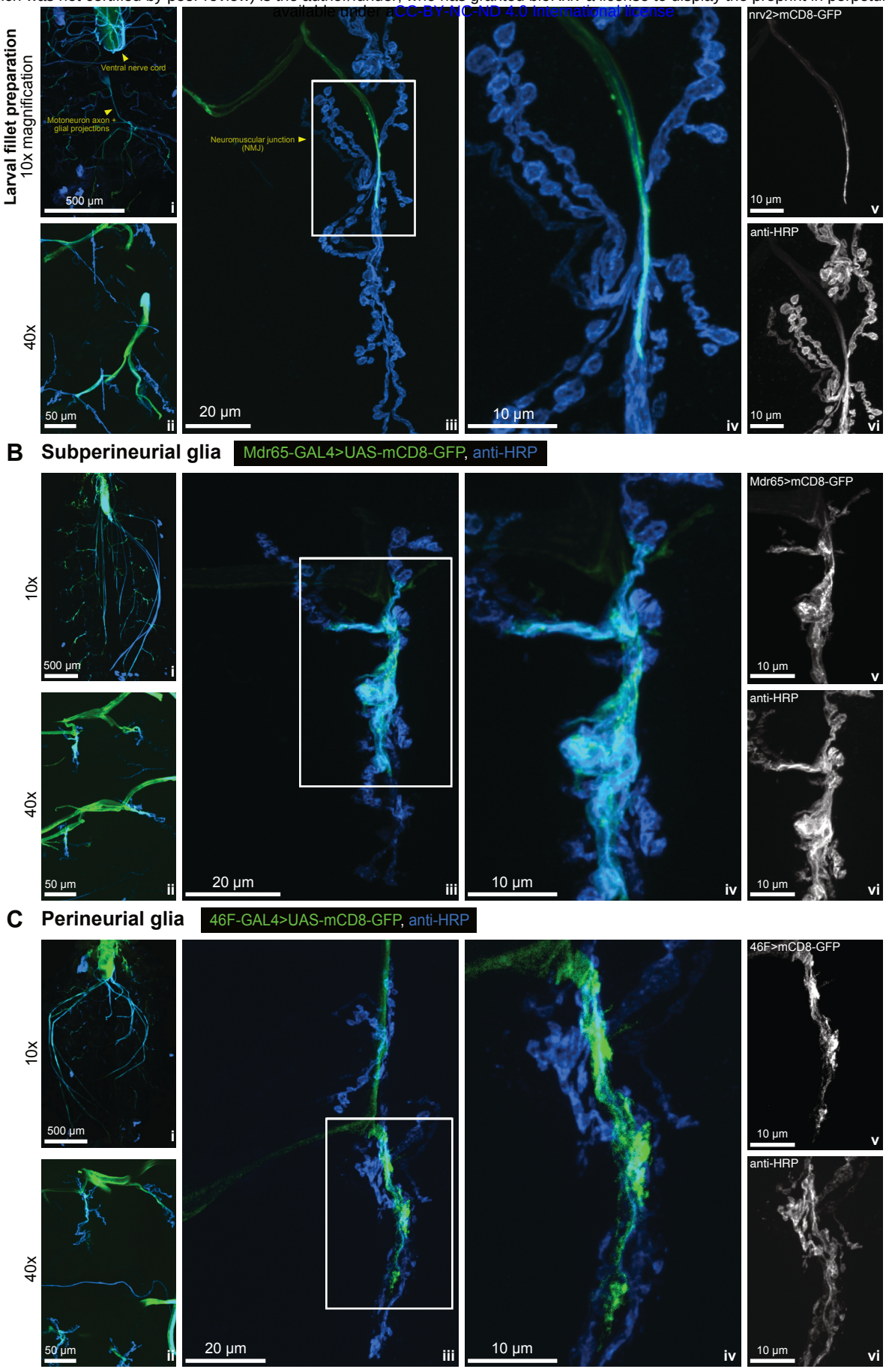

# Figure 4



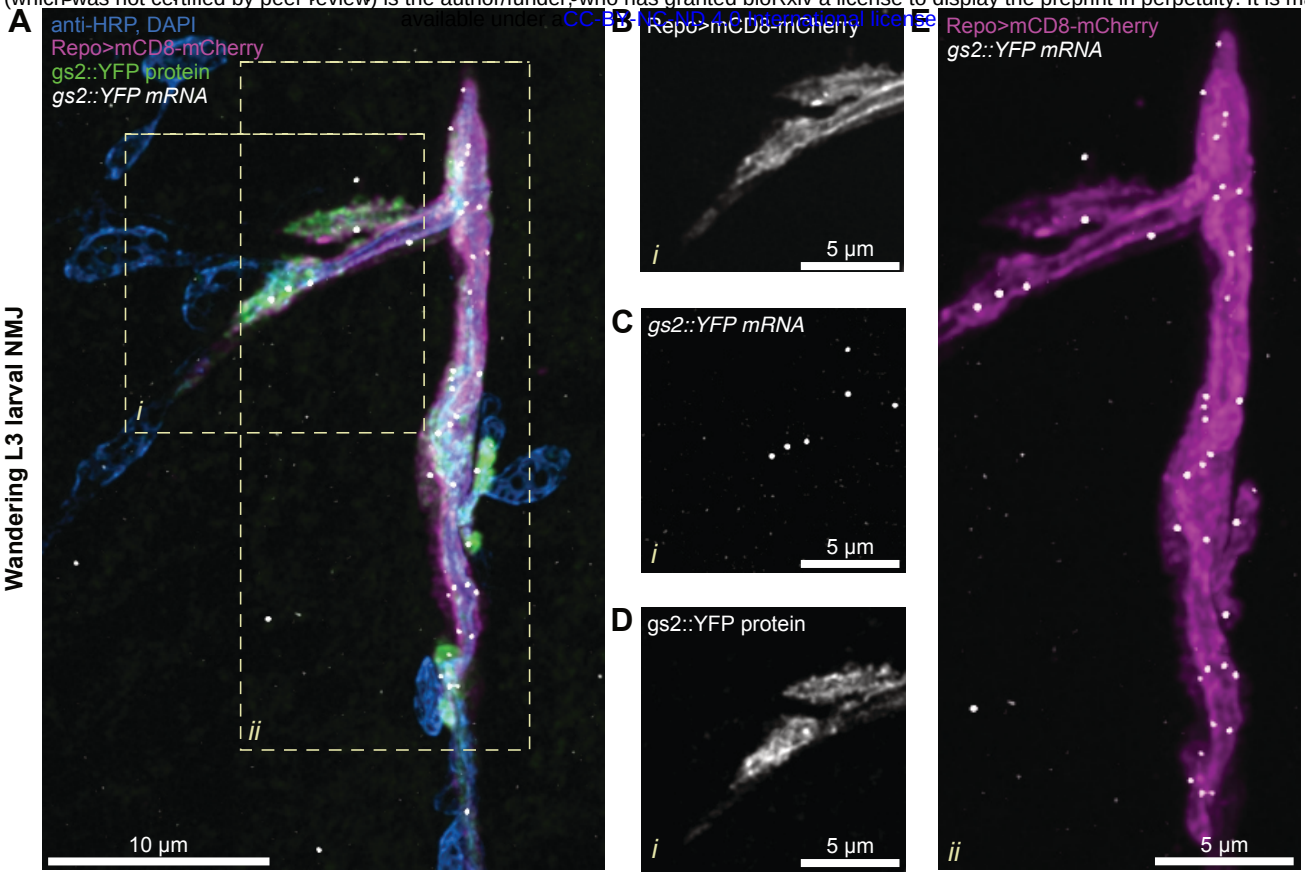

# Figure S4



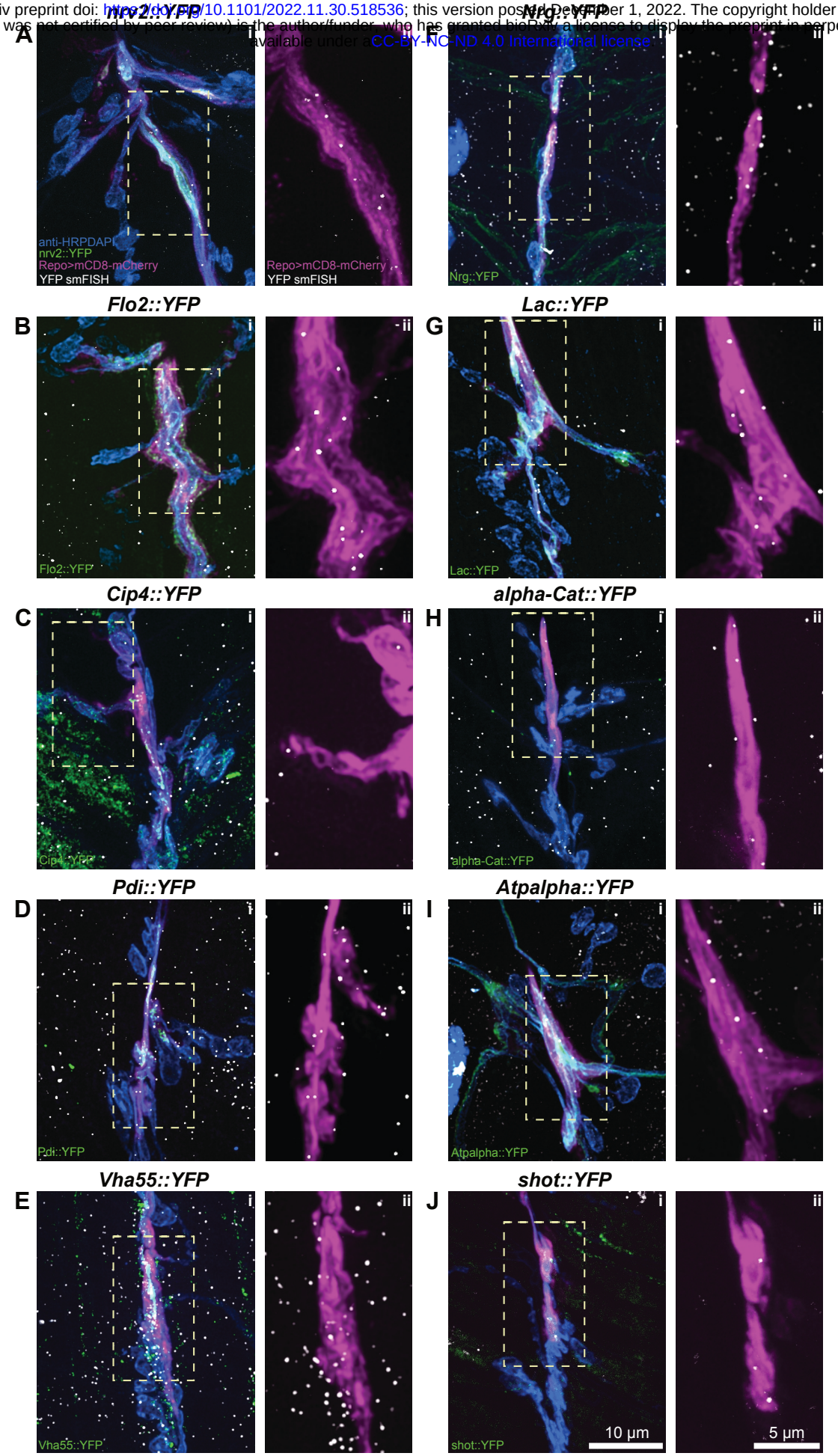

# Figure 2



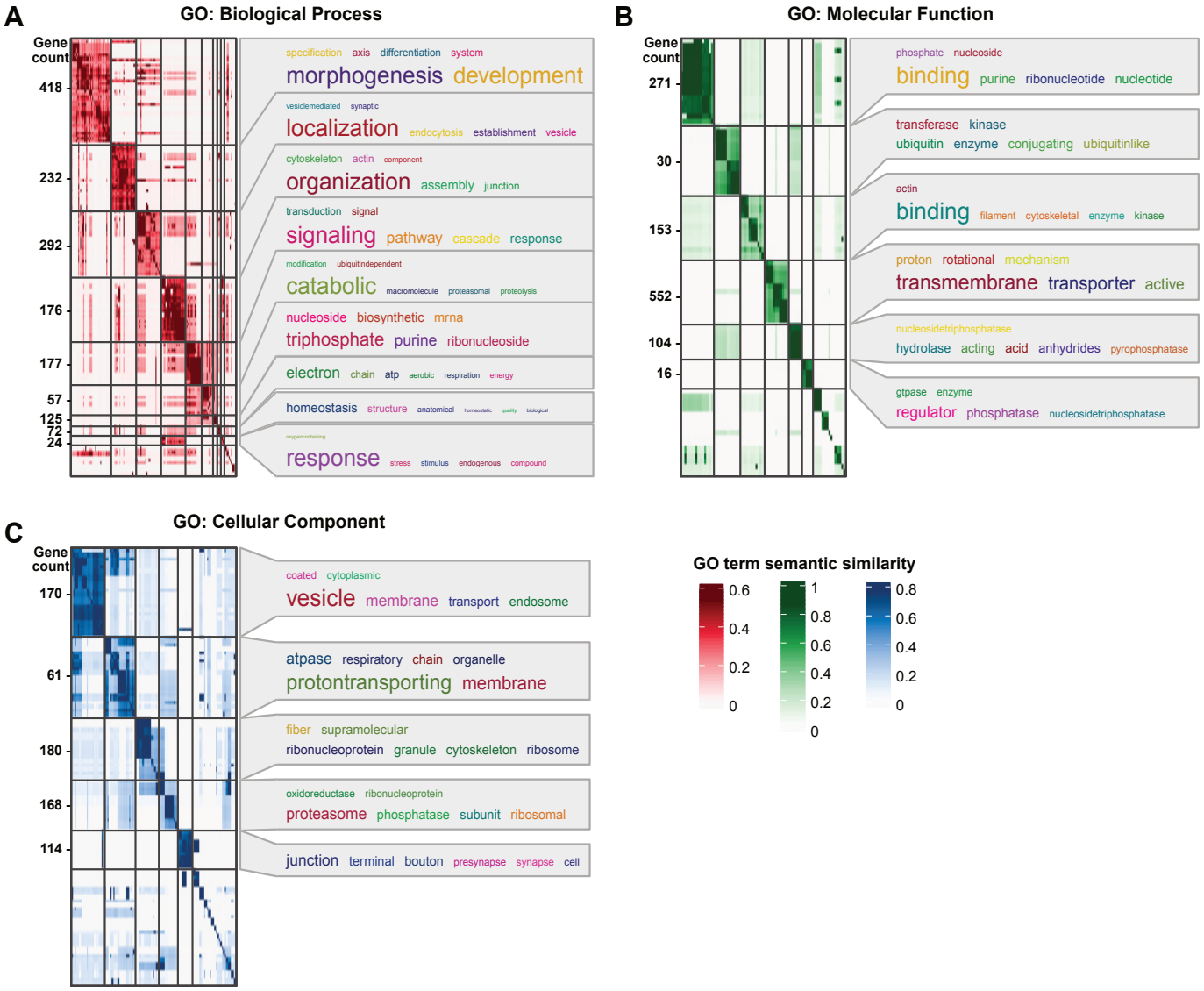

# Figure S2



**Gene Ontology enrichment of 1700 glia-localised transcripts**
Half-volcano plot - Top 20 (foldchange) terms are labelled

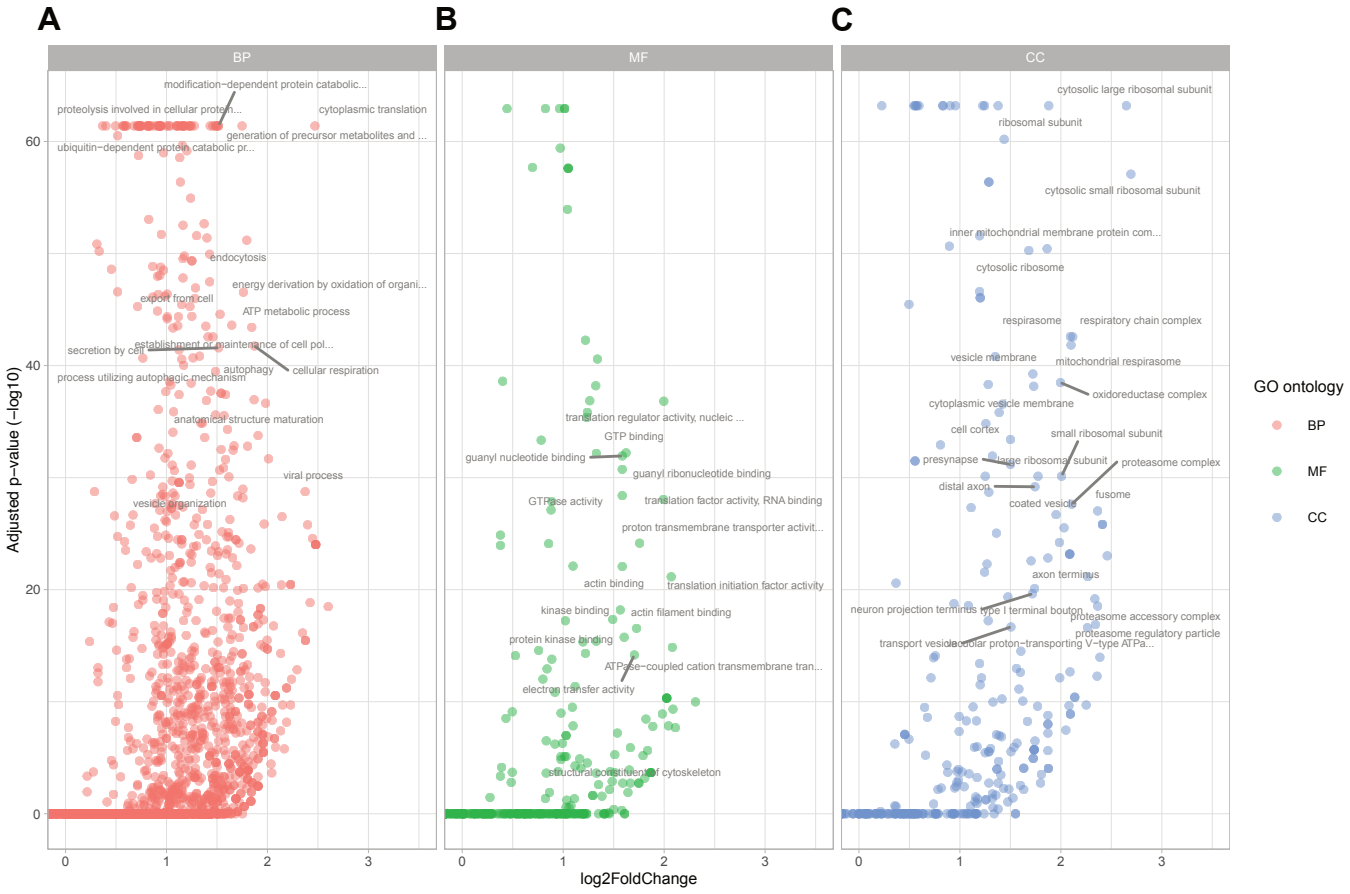

# Figure 3



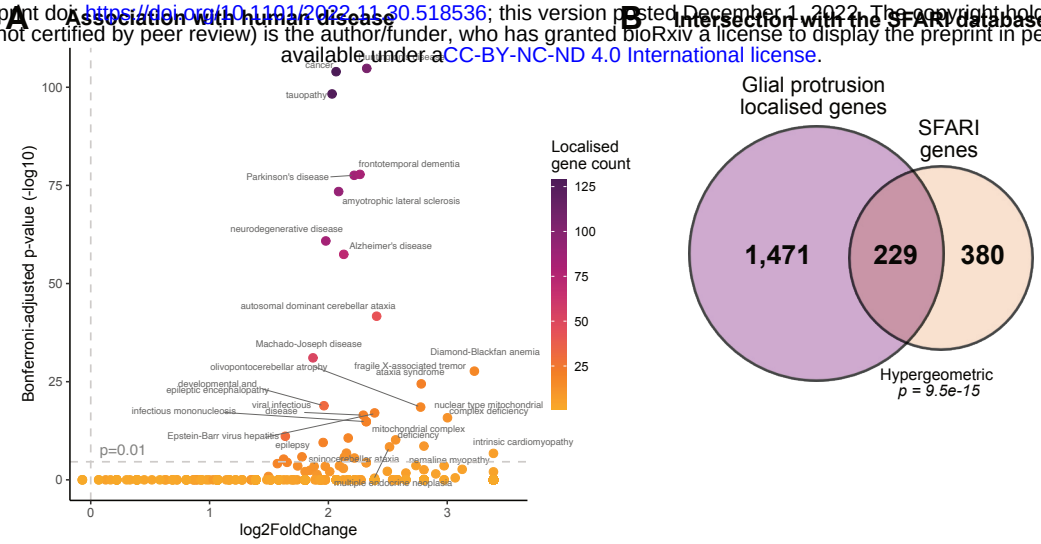


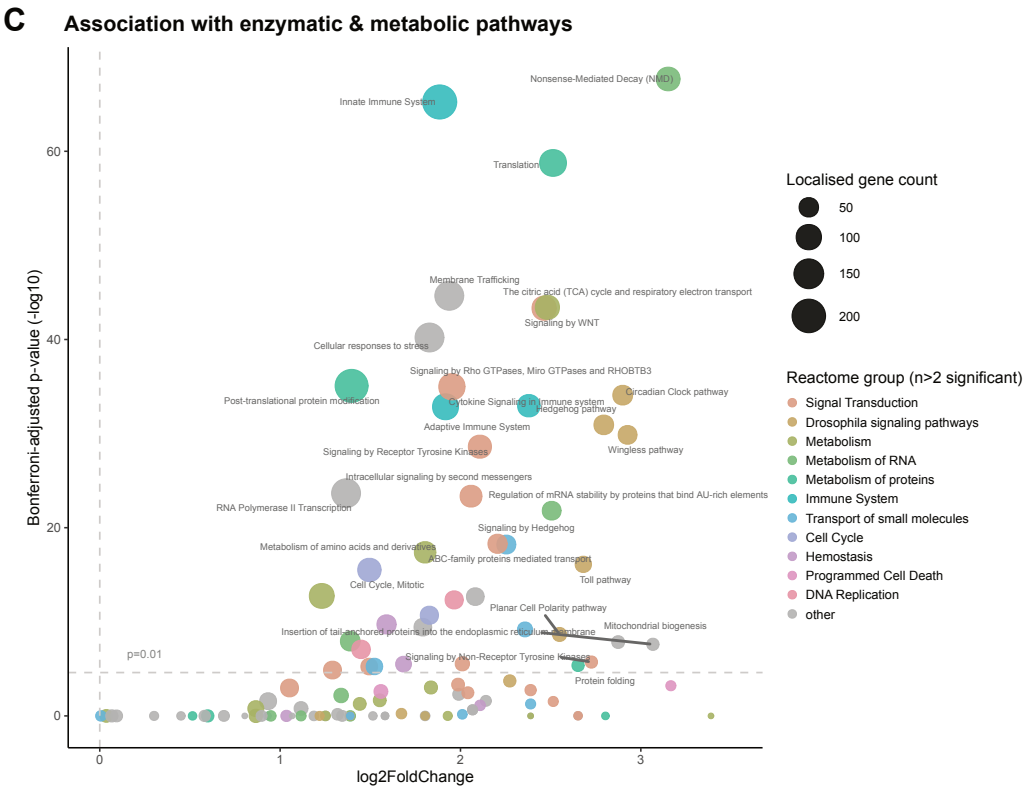

# Figure 5



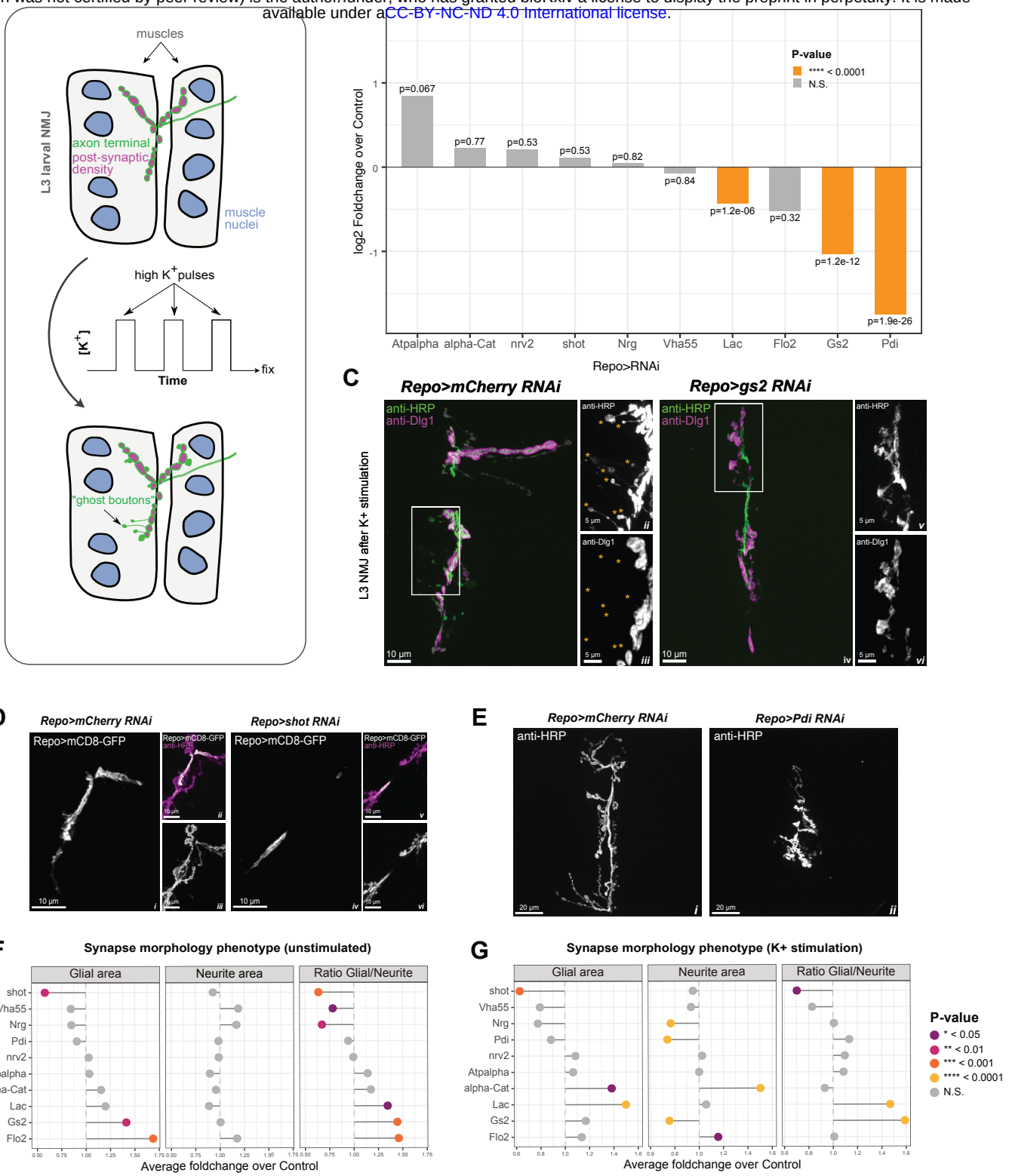

# Figure S5